

The synthesis of, and characterization of the dynamic processes occurring in Pd(II) chelate complexes of 2-pyridyldiphenylphosphine†

Jianke Liu, Chacko Jacob, Kelly J. Sheridan, Firas Al-Mosule, Brian T. Heaton, Jonathan A. Iggo,* Mark Matthews, Jeremie Pelletier, Robin Whyman, Jamie F. Bickley and Alexander Steiner

Received 3rd September 2009, Accepted 4th June 2010

First published as an Advance Article on the web 26th July 2010

DOI: 10.1039/b918162h

Pd(II) complexes in which 2-pyridyldiphenylphosphine (Ph₂Ppy) chelates the Pd(II) centre have been prepared and characterized by multinuclear NMR spectroscopy and by X-ray crystallographic analysis. *trans*-[Pd(κ¹-Ph₂Ppy)₂Cl₂] is transformed into [Pd(κ²-Ph₂Ppy)(κ¹-Ph₂Ppy)Cl]Cl by the addition of a few drops of methanol to dichloromethane solutions, and into [Pd(κ²-Ph₂Ppy)(κ¹-Ph₂Ppy)Cl]X by addition of AgX or TlX, (X = BF₄⁻, CF₃SO₃⁻ or MeSO₃⁻). [Pd(κ¹-Ph₂Ppy)₂(*p*-benzoquinone)] can be transformed into [Pd(κ²-Ph₂Ppy)(κ¹-Ph₂Ppy)(MeSO₃)]₂[MeSO₃] by the addition of two equivalents of MeSO₃H. Addition of further MeSO₃H affords [Pd(κ²-Ph₂Ppy)(κ¹-Ph₂PpyH)(MeSO₃)]₂[MeSO₃]₂. Addition of two equivalents of CF₃SO₃H, MeSO₃H or CF₃CO₂H and two equivalents of Ph₂Ppy to [Pd(OAc)₂] in CH₂Cl₂ or CH₂Cl₂–MeOH affords [Pd(κ²-Ph₂Ppy)(κ¹-Ph₂Ppy)X]X, (X = CF₃SO₃⁻, MeSO₃⁻ or CF₃CO₂⁻), however addition of two equivalents of HBF₄·Et₂O affords a different complex, tentatively formulated as [Pd(κ²-Ph₂Ppy)₂]X₂. Addition of excess acid results in the clean formation of [Pd(κ²-Ph₂Ppy)(κ¹-Ph₂PpyH)(X)]X₂. In methanol, addition of MeSO₃H and three equivalents of Ph₂Ppy to [Pd(OAc)₂] affords [Pd(κ²-Ph₂Ppy)(κ¹-Ph₂Ppy)₂][MeSO₃]₂ as the principal Pd-phosphine complex. The fluxional processes occurring in these complexes and in [Pd(κ¹-Ph₂Ppy)₃Cl]X, (X = Cl, OTf) and the potential for hemilability of the Ph₂Ppy ligand has been investigated by variable-temperature NMR. The activation entropy and enthalpy for the regioselective fluxional processes occurring in [Pd(κ²-Ph₂Ppy)(κ¹-Ph₂Ppy)₂][MeSO₃]₂ have been determined and are in the range –10 to –30 J mol⁻¹ K⁻¹ and *ca.* 30 kJ mol⁻¹ respectively, consistent with associative pathways being followed. The observed regioselectivities of the exchanges are attributed to the constraints imposed by microscopic reversibility and the small bite angle of the Ph₂Ppy ligand. X-Ray crystal structure determinations of *trans*-[Pd(κ¹-Ph₂Ppy)₂Cl₂], [Pd(κ²-Ph₂Ppy)(κ¹-Ph₂Ppy)Cl][BF₄], [Pd(κ¹-Ph₂Ppy)₂(*p*-benzoquinone)], *trans*-[Pd(κ¹-Ph₂PpyH)₂Cl₂][MeSO₃]₂, and [Pd(κ¹-Ph₂Ppy)₃Cl](Cl) are reported. In [Pd(κ²-Ph₂Ppy)(κ¹-Ph₂Ppy)Cl][BF₄] a donor–acceptor interaction is seen between the pyridyl-N of the monodentate Ph₂Ppy ligand and the phosphorus of the chelating Ph₂Ppy resulting in a trigonal bipyramidal geometry at this phosphorus.

Introduction

The coordination chemistry of chelating ligands containing mixed functionalities at transition-metal centres is an extremely active area of research since the presence of two different donor groups should allow tuning of the coordination chemistry and hence functionality of the resulting complexes.^{1–5} For example, the catalytic utility of hemilabile ligands has received considerable attention since the presence of a weakly chelating group, capable

of coordinating temporarily to a transition-metal centre in the absence of substrate, but that in the presence of substrate, can be readily displaced to give a metal–substrate complex, offers the potential for effective stabilization of the metal centre without compromising its activity. The substitutionally inert portion of these ligands can be used to tune the selectivity of the transition-metal centre and the presence of the labile donor group may allow this part of the ligand to play a dual role, both as a donor group when required and *via* a “secondary interaction” such as a proton transfer agent when decoordinates from the metal.^{6,7} Hemilabile ligands have indeed been successfully employed in a range of catalytic reactions, including methanol carbonylation, hydrogenation, hydroformylation and polymerisation of ethene with CO.⁴ A common combination of donor functionalities in such ligands is a phosphine with a nitrogen donor; such ligands have shown promise in many catalytic reactions.^{2,8–15} For example, Drent and co-workers,^{16,17} reported Pd systems incorporating pyridylphosphine ligands which show activities three or more orders of magnitude greater than analogous phosphine based systems even under considerably milder conditions (318 vs. 388 K).^{7,17} Drent attributed this remarkable increase in activity

Department of Chemistry, Donnan and Robert Robinson Laboratories, University of Liverpool, P. O. Box. 147, Liverpool, UK, L69 7ZD. E-mail: iggo@liv.ac.uk; Fax: 44 (0)151 794 3588; Tel: 44 (0)151 794 3538

† Electronic supplementary information (ESI) available: NMR spectra of the complexes and simulations of the variable-temperature data. Eyring and Arrhenius plots for the dynamic processes in [Pd(κ²-Ph₂Ppy)(κ¹-Ph₂Ppy)Cl](Cl), [Pd(κ²-Ph₂Ppy)(κ¹-Ph₂Ppy)Cl][OTf], [Pd(κ²-Ph₂Ppy)(κ¹-Ph₂Ppy)₂][MeSO₃]₂ and [Pd(κ¹-Ph₂Ppy)₃Cl][CF₃SO₃]. Crystal data and structure refinement for *trans*-[Pd(κ¹-Ph₂Ppy)₂Cl₂], *trans*-[Pd(κ¹-Ph₂PpyH)₂Cl₂][MeSO₃]₂, [Pd(κ²-Ph₂Ppy)(κ¹-Ph₂Ppy)Cl][BF₄], [Pd(κ¹-Ph₂Ppy)₂(benzoquinone)] and [Pd(κ¹-Ph₂Ppy)₃Cl](Cl). CCDC reference numbers 746623–746627. For ESI and crystallographic data in CIF or other electronic format see DOI: 10.1039/b918162h

to the ability of Ph₂Ppy to act as a proton relay. An additional possibility is that Ph₂Ppy acts as a hemilabile ligand to stabilize the catalyst.¹⁷ Drent's initial report has been followed by several others exploring new P,N-bidentate ligands^{18–23} and the mechanism of the catalysis.^{7,17,22,24–27} Elsevier has recently developed variants of the pyridylphosphine ligand for catalysis in supercritical CO₂²² and Doherty has described polymer bound Pd/pyridylphosphine catalysts.²⁸

The explanation for the enhanced catalytic activity of Ph₂Ppy vs. PPh₃ is still open to debate since a general consensus regarding the catalytic reaction mechanism has, as yet, not been reached with both Pd(0)^{13–15} and Pd(II)^{7,17,25} intermediates being proposed in which the pyridylphosphine ligands adopt monodentate,^{24–26} or mixed mono- and bi-dentate^{7,17} coordination, or in which the coordination mode of the ligand is not defined.²⁷ Thus, although there appears general agreement that the ligand *may* act as a proton relay, the possibility that the hemilability of the ligand is also important has received little attention, indeed the coordination chemistry of 2-pyridyldiphenylphosphine with palladium(II) and the potential for hemilability of Ph₂Ppy at Pd(II) has been little explored.³

Our interest in Pd/phosphine catalyzed hydrocarboxylation of alkenes and alkynes has led us to investigate the chemistry of the potentially hemilabile 2-pyridyldiphenylphosphine ligand (Ph₂Ppy) at Pd(II). Transition-metal complexes of pyridylphosphine ligands have been well known for many years.³ Although both monodentate and bridging coordination modes of pyridylphosphines to Pd(II), and chelating coordination to other transition metals are well documented, it is surprising that examples of a pyridylphosphine ligand chelating a Pd(II) centre are rare.²⁹ In palladium(II) chemistry, monodentate complexes are usually formed by the binding of the soft phosphorus atom to the metal centre; no N-bound monodentate complexes have been reported and there are only two previous reports of κ²-pyridylphosphine chelating complexes of Pd(II) – [Pd(κ²-Me₂Ppy)(κ¹-Me₂Ppy)X]Y, (X = Cl, Br, I, Y = [ClO₄], [PF₆])³⁰ and the pyrimidylphosphine complex [Pd{κ²-Ph₂P(C₄H₃N₂)₂}[BF₄]₂.²⁰ The X-ray crystal structures of the small number of chelating four-membered ring complexes containing Ph₂Ppy (at metals other than Pd(II)), reveal a highly compressed P–M–N angle of *ca.* 70°.^{29–32} Within the chelate ring, there is also significant angular compression. Both the C–N–M and the N–C–P angles are reduced from the ideal value of 120° and the C–P–M angle is reduced below the expected value of 109.5°. Furthermore, the chelate P–C distance is longer than the non-chelate P–C distances. The ring strain in these chelated complexes render them unstable, thus the nitrogen donor is readily displaced from the low-valent metal giving phosphorus bound monodentate complexes.⁵ In many instances binuclear complexes in which the ligand bridges the metal–metal bond are preferred.^{31–40}

Results and discussion

Synthesis of Pd(II) complexes with both chelating and monodentate Ph₂Ppy ligands

Direct addition of Ph₂Ppy to [Pd(PhCN)₂Cl₂] in dichloromethane solution, (metal:ligand ratio varied from 4:1 to 1:2) gave a mixture of three complexes each of which shows a sharp singlet in

the ³¹P{¹H} NMR spectrum (Supplementary Fig. 1, ESI†). The two high frequency resonances, δ(P) 29.0 and 22.8 ppm, indicate Ph₂Ppy ligands bound through phosphorus only (*cf.* that of the free ligand δ(P) –4.5 ppm),³ whilst the extremely low frequency chemical shift of the third resonance, δ(P) –61.6 ppm, is characteristic for this ligand in a strained, four-membered chelate ring.⁴¹ The absence of coupling indicates one type of phosphorus is present in each complex consistent with the formulations [Pd(κ²-Ph₂Ppy)Cl₂] (**1**), *cis*-[Pd(κ¹-Ph₂Ppy)₂Cl₂] (**2a**) (δ(P) 29.0 (s) ppm), and *trans*-[Pd(κ¹-Ph₂Ppy)₂Cl₂] (**2b**) (δ(P) 22.8 (s) ppm).^{34,37,39,42,43} A mixture of *cis*- and *trans*-[Pd(κ¹-Ph₂Ppy)₂Cl₂] (**2a/b**) can be obtained analytically pure and in high yield as a yellow solid by treatment of [Pd(PhCN)₂Cl₂] in dichloromethane with 2 equivalents of Ph₂Ppy, followed by precipitation with diethyl ether as previously reported by Balch *et al.*³⁸ [Pd(COD)Cl₂] and [Pd(TMEDA)Cl₂] can also be used as the palladium source in the reaction. Yellow crystals, suitable for an X-ray crystal structure determination were obtained by layering a dichloromethane solution of a mixture of *cis* and *trans* isomers **2a/b** with diethyl ether (see ESI†). Visually, there appeared to be only one type of crystal present,⁴⁴ which the X-ray determination showed to contain the *trans* isomer **2b** (Supplementary Fig. 44, Supplementary Table 3, ESI†). However, the ³¹P{¹H} NMR spectrum recorded immediately on dissolution of the crystals showed a mixture of **2a** and **2b**. This seems surprising in view of the sharpness of both resonances, indicating that interconversion of the isomers is slow on the NMR timescale at 293 K. The proportions of **2a** and **2b** present in solution is temperature dependent. For example in CD₂Cl₂ the ratio **2a** : **2b** is 70 : 30 at 293 K and 97 : 3 at 193 K. Furthermore, Balch has reported that it is the *cis* and not the *trans* complex that is involved in the exchange process in the analogous platinum system.³⁷ Anion assisted fluxional processes in these systems are discussed later and might account for the rapid interconversion of *trans* and *cis* isomers.

Balch *et al.*⁴⁵ have previously reported the existence of an equilibrium between *cis*-[Pt(κ¹-Ph₂Ppy)₂X₂] (X = I, Cl) and “chelate–monodentate” [Pt(κ²-Ph₂Ppy)(κ¹-Ph₂Ppy)X](X) (X = I, Cl) in chloroform solution. The position of the equilibrium shifts in favour of the cationic “chelate–monodentate” complex at low temperature, which is attributed to the entropic contribution of two monodentate Ph₂Ppy ligands vs. one monodentate Ph₂Ppy ligand becoming less significant at low temperature. Thus, ionization of halide from the platinum centre in [Pt(Ph₂Ppy)₂X₂] (assisted by intramolecular attack of a pyridyl nitrogen) in chloroform solution is feasible. This may reflect the greater propensity of square-planar platinum complexes to react by a dissociative pathway.⁴⁶ By contrast, we see no evidence for the formation of a “chelate–monodentate” structure from the palladium complexes **2a/b** in dichloromethane at low temperatures.

There are a few reports of the formation of P,N chelates, including the closely related complexes [Pt(κ²-Ph₂Ppy)(κ¹-Ph₂Ppy)Cl][Rh(CO)₂Cl₂],³¹ and [Pd(κ²-Me₂Ppy)(κ¹-Me₂Ppy)X](Y), (X = Cl, Br, I, Y = [ClO₄], [PF₆])³⁰ and [Pt(κ²-Ph₂Ppy)(κ¹-Ph₂Ppy)X][BPh₄]²⁹ the latter complexes being prepared by halide abstraction using silver salts from dihalide complexes [ML₂X₂]. This approach proved unsuccessful here.

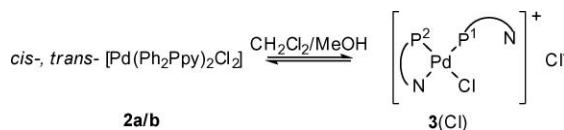
However, we find that addition of a few drops of MeOH to a dichloromethane suspension of **2a/b** results in complete dissolution of the solid. ³¹P{¹H} NMR spectroscopy revealed the

Table 1 $^{31}\text{P}\{^1\text{H}\}$ NMR data for Pd(II)–Ph₂Ppy compounds at 193 K in dichloromethane unless otherwise stated^a

Compound	$\delta(\text{P}^1)^b/\text{ppm}$	$\delta(\text{P}^2)^b/\text{ppm}$	$\delta(\text{P}^3)/\text{ppm}$	$^2J(\text{P}^1\text{--P}^2)/\text{Hz}$	$^2J(\text{P}^2\text{--P}^3)/\text{Hz}$
1	[Pd(κ^2 -Ph ₂ Ppy)Cl ₂]	—	−61.6 s	—	—
2a	<i>cis</i> -[Pd(Ph ₂ Ppy) ₂ Cl ₂] ^c	29.0 s	—	—	—
2b	<i>trans</i> -[Pd(Ph ₂ Ppy) ₂ Cl ₂] ^c	22.8 s	—	—	—
2[CF₃CO₂]	[Pd(κ^1 -Ph ₂ Ppy) ₂ (CF ₃ CO ₂) ₂]	27.6 br	—	—	—
2b'	<i>trans</i> -[Pd(Ph ₂ PpyH) ₂ Cl ₂][MeSO ₃] ₂ ^d	19.1 s	—	—	—
3(Cl)	[Pd(κ^2 -Ph ₂ Ppy)(κ^1 -Ph ₂ Ppy)Cl](Cl) ^{de}	44.4 d	−44.0 d	—	33.0
3[BF₄]	[Pd(κ^2 -Ph ₂ Ppy)(κ^1 -Ph ₂ Ppy)Cl][BF ₄] ^{de}	44.8 d	−43.8 d	—	38.2
3[OTf]	[Pd(κ^2 -Ph ₂ Ppy)(κ^1 -Ph ₂ Ppy)Cl][OTf] ^{de}	44.6 d	−43.9 d	—	38.1
3[MeSO₃]	[Pd(κ^2 -Ph ₂ Ppy)(κ^1 -Ph ₂ Ppy)Cl][MeSO ₃]	44.7 d	−43.8 d	—	38.2
4(Cl)	[Pd(κ^1 -Ph ₂ Ppy) ₃ Cl](Cl) ^{ef†}	33.1 br	—	25.7 br	—
4[OTf]	[Pd(κ^1 -Ph ₂ Ppy) ₃ Cl][OTf] ^{ef†}	33.2 br	—	25.6 br	—
7	[Pd(κ^1 -Ph ₂ Ppy) ₂ (<i>p</i> -benzoquinone)]	30.2 s	—	—	—
8[OTf]	[Pd(κ^2 -Ph ₂ Ppy)(κ^1 -Ph ₂ Ppy)(OTf)][OTf]	40.8 d	−39.3 d	—	Unresolved
8[MeSO₃]	[Pd(κ^2 -Ph ₂ Ppy)(κ^1 -Ph ₂ Ppy)(MeSO ₃)] ₂	41.2 d	−40.0 d	—	29.8
8[CF₃CO₂]	[Pd(κ^2 -Ph ₂ Ppy)(κ^1 -Ph ₂ Ppy)(CF ₃ CO ₂)] ₂	40.8 d	−38.6 d	—	24.4
8'[OTf]	[Pd(κ^2 -Ph ₂ Ppy)(κ^1 -Ph ₂ PpyH)(OTf)][OTf] ₂	26.4	−45.0	—	—
8'[MeSO₃]	[Pd(κ^2 -Ph ₂ Ppy)(κ^1 -Ph ₂ PpyH)(MeSO ₃)] ₂	26.0 br	−45.8 br	—	Unresolved
8[BF₄]	[Pd(κ^2 -Ph ₂ Ppy)(κ^1 -Ph ₂ PpyH)(BF ₄)] ₂	25.2	−43.7	—	—
9	[Pd(κ^2 -Ph ₂ Ppy) ₂][BF ₄]	—	−42.9 br	—	—
10	[Pd(κ^2 -Ph ₂ Ppy)(κ^1 -Ph ₂ Ppy) ₂][MeSO ₃] ₂ ^g	44.7 s br	−47.7 d br	23.6 d br	Unresolved 388

^a See Experimental section for ^1H and ^{19}F NMR. ^b See Scheme 1 for numbering scheme. ^c At 293 K. ^d In dichloromethane–MeOH solution. ^e At 233 K. ^f P1 *trans* to Cl, see Supplementary Fig. 37, ESI†. ^g See Scheme 4 for numbering scheme.

formation of the cationic Pd(II) “chelate–monodentate” complex [Pd(κ^2 -Ph₂Ppy)(κ^1 -Ph₂Ppy)Cl](Cl), **3(Cl)** (Scheme 1). Thus, the $^{31}\text{P}\{^1\text{H}\}$ NMR spectrum of **3(Cl)** at 233 K shows two sets of doublets at $\delta(\text{P})$ 44.4 (d) and −44.0 (d) ppm, $^2J(\text{P}^1\text{--P}^2) = 33.0$ Hz indicating the presence of two mutually *cis*, inequivalent phosphorus atoms, Table 1 (Supplementary Fig. 2a, ESI†). The resonance at very low frequency can be assigned on the basis of its chemical shift to the phosphorus of a chelating Ph₂Ppy ligand⁴¹ with P *trans* to Cl, P² in Scheme 1. The resonance at high frequency ($\delta(\text{P})$ 44.4 ppm) is consequently assigned to the phosphorus of a monodentate pyridylphosphine ligand *trans* to the chelating nitrogen of the pyridine ring, P¹ in Scheme 1. The breadth of the resonances at 293 K is attributed to counterion assisted displacement of the coordinated chloride ligand by nitrogen (*vide infra*). The “chelate–monodentate” structure of **3** has been confirmed by an X-ray crystal structure determination of [Pd(κ^2 -Ph₂Ppy)(κ^1 -Ph₂Ppy)Cl][BF₄], **3[BF₄]** which can be obtained as an analytically pure yellow powder by addition of 1 equivalent of Ag[BF₄] to a dichloromethane–MeOH (8 : 1) solution of **3(Cl)**, followed by precipitation with excess ether.



Scheme 1 Synthetic route to the ionic Pd(II) “chelate–monodentate” complex **3(Cl)**.

Salts of **3** with other counterions can be prepared by the addition of one to four equivalents of TIX to a dichloromethane solution of **2** or to a dichloromethane–methanol solution of **3(Cl)**, to give **3(X)**, (X = BF₄, OTf, MeSO₃). The $^{31}\text{P}\{^1\text{H}\}$ NMR spectra of **3(X)** in CH₂Cl₂ at 233 K are essentially independent of X, showing two sharp doublets at $\delta(\text{P})$ 44.7 and −43.8 (± 0.1) ppm with $^2J(\text{P}^1\text{--P}^2) = 38.2$ Hz with only small counterion dependent shifts of the

resonances, Table 1 (Supplementary Fig. 2a, ESI†). However, the dynamic behaviour of the NMR spectra is counterion dependent, *e.g.* the VT spectra of **3(Cl)** show significant broadening as the temperature is raised to 293 K, whereas those of **3[BF₄]** remain sharp, Supplementary Fig. 2a and b, ESI†. This dynamic behaviour is discussed later.

Crystal structure of [Pd(κ^2 -Ph₂Ppy)(κ^1 -Ph₂Ppy)Cl][BF₄] (3[BF₄]**).** Crystals of **3[BF₄]** suitable for an X-ray crystal structure determination were obtained by layering a dichloromethane solution of **3[BF₄]** with diethyl ether. Fig. 1 shows a representation of **3[BF₄]**, selected bond lengths and angles are given in Table 2.

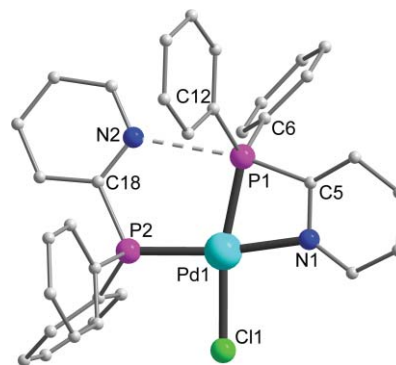


Fig. 1 Molecular structure of [Pd(κ^2 -Ph₂Ppy)(κ^1 -Ph₂Ppy)Cl][BF₄] (**3[BF₄]**), with H atoms removed for clarity.

The coordination about the palladium is distorted square planar. One of the pyridylphosphine ligands chelates the Pd through nitrogen and phosphorus while the other functions as a monodentate phosphorus bound ligand. The two phosphorus atoms are mutually *cis* in agreement with the $^{31}\text{P}\{^1\text{H}\}$ NMR spectrum recorded in solution. The Pd–P bonds have essentially the same lengths, 2.2644(4) and 2.2330(4) Å. The Pd–N bond length is 2.1075(2) Å, in agreement with the closely related cation

Table 2 Selected bond lengths (Å) and angles (°) for [Pd(κ^2 -Ph₂Ppy)(κ^1 -Ph₂Ppy)Cl][BF₄] (**3**[BF₄])

Pd–P1	2.2644(4)	Pd–P2	2.2330(4)
Pd–N1	2.1075(2)	Pd–Cl1	2.3225(5)
P2–Pd–P1	101.666(14)	N1–Pd–Cl1	97.54(3)
P2–Pd–Cl1	90.134(14)	N1–Pd–P1	70.45(3)
P1–C5–N1	103.38(10)	P1–C5–C4	134.24(11)
N1–C5–C4	122.30(13)	N2–C18–P2	117.01(11)
C5–N1–C1	120.13(13)	Pd–N1–C1	136.20(10)
C5–N1–Pd	101.73(9)	C5–P1–Pd	82.63(5)
N1–Pd–P2	168.19(3)	P1–Pd–Cl1	167.983(15)

[Pd(κ^2 -Me₂Ppy)(κ^1 -Me₂Ppy)Cl]⁺.³⁰ A terminal chloride ligand completes the coordination sphere. The presence of a strained four-membered chelate ring results in the interbond angles at palladium deviating strongly from the ideal value of 90°.

Thus, P1–Pd–N1 is only 70.45°. This compression causes the two adjacent angles to open up, N1–Pd–Cl1 is 97.54° and P1–Pd–P2 is 101.66°. The P2–Pd–Cl1 angle is 90.13°, close to the ideal value. There is also significant angular compression within the chelate ring. Thus, C5–N1–Pd and P1–C5–N1 are 101.73 and 103.38°, respectively, reduced from an ideal 120° and the C5–P1–Pd angle is 82.63°, reduced from the expected value of 109.5°. The angular compression seen in this ring is very similar to that found in the chelate ring of [Pt(κ^2 -Ph₂Ppy)(κ^1 -Ph₂Ppy)Cl]⁺.³¹ In addition, there is a weak donor acceptor interaction between the phosphorus centre of the chelating ligand and the nitrogen atom of the monodentate phosphine. The distance P1...N2 is 2.7472(14) Å, which is well below the sum of their van der Waals radii of 3.35 Å.⁴⁷ The P1...N2 interaction is accompanied by a wider Ph–P–Ph angle [C(Ph)–P1–C(Ph) 111.28(7) and C(Ph)–P2–C(Ph) 108.01(7) Å]. This interligand interaction appears to optimise the ligand packing within the square planar coordination sphere. A search of the Cambridge Structural Database revealed that short interligand P...N contacts between dangling pyridines and metal-coordinating phosphines are not uncommon but have not previously been noted in the relevant literature. For example, the corresponding Pt-complex [Pt(κ^2 -Ph₂Ppy)(κ^1 -Ph₂Ppy)Cl]⁺ exhibits an even shorter interligand P...N interaction of 2.67 Å (in conjunction with a significantly wider Ph–P–Ph angle of 115.4° at the N-interacting phosphorus centre).³¹ The P...N interaction between dppm and one pyridine-2-thiolate ligand in [Pt(κ^2 -dppm)(κ^1 -py-2-S)₂] is similarly short.⁴⁸ Incidentally, the latter features the largest Ph–P–Ph angle (114.5°) of all structurally characterized square planar Pd- and Pt-dppm complexes (mean 106.5°).

Reaction of 3 with donor substrates. The nitrogen of the chelate ring can be displaced in methanol–dichloromethane solution by addition of another equivalent of Ph₂Ppy to give [Pd(κ^1 -Ph₂Ppy)₃Cl](Cl) (**4**(Cl)) which can be converted to the triflate salt [Pd(κ^1 -Ph₂Ppy)₃Cl][OTf] (**4**(OTf)) by reaction with Tf[OTf]. Reaction with Ag[BF₄] affords a complex mixture which includes silver–Ph₂Ppy complexes;⁴⁹ this mixture has not been further characterized. The formation of silver complexes presumably reflects the labile nature of the Ph₂Ppy ligands in **4**. The ³¹P{¹H} NMR spectrum of **4**(Cl) shows a single, very broad resonance around 26 ppm at 293 K. On cooling the solution, the resonances sharpen between 273 and 223 K then broaden again below 223 K

becoming very broad at 193 K (Supplementary Fig. 32, ESI†). The ¹H NMR spectra of **4**(Cl) show similar VT behaviour becoming very broad at low temperature and are uninformative. At 233 K the ³¹P{¹H} NMR spectrum shows two resonances of intensity 1 : 2 at δ (P) = 33.1 and 25.7 ppm as expected. Couplings between the resonances are not resolved, although shoulders are just discernible on the resonance of **4**(OTf) at δ (P) = 33.2 ppm at 233 K, consistent with a triplet due to coupling to two equivalent phosphorus nuclei, ²J(PP) < 8 Hz. At 193 K at least three resonances can be distinguished at ca. 32.4, 27.4 and 25.2 ppm, indicating a very dynamic system in which the *trans* disposed Ph₂Ppy ligands become inequivalent to each other. These dynamic processes are discussed later. Attempted precipitation of **4**(Cl) by addition of diethylether afforded an impure mixture of **2a**, **2b** and free Ph₂Ppy. However, slow removal of solvent at reduced pressure afforded crystals of **4**(Cl) suitable for an X-ray crystal structure determination (see ESI†). **4**(OTf) can be precipitated in diethyl ether and redissolved in e.g. CDCl₃.

Other strongly coordinating ligands such as Cl[−] and PPh₃ also disrupt the four-membered chelate in **3**(Cl) although the resultant ³¹P{¹H} NMR spectra show a mixture of unidentifiable products. However, other potential donors relevant to alkyne hydroesterification catalytic systems appear not to disrupt the chelate structure readily. Thus, bubbling CO through a dichloromethane–MeOH solution of **3**(Cl) at 293 K and ambient pressure does not result in displacement of the chelating nitrogen. Liu *et al.* has previously commented on the relatively low affinity of CO for Pd(II) centres in these systems.^{50,51} Neither is the nitrogen displaced by MeC≡CH or PhC≡CH.

Preparation of “chelate–monodentate” complexes by halide abstraction. The presence of a tightly bound halide ligand in the fourth coordination site at Pd(II) has been observed to suppress strongly the activity of the Pd centre in organometallic catalytic reactions. Thus, for example, van Leeuwen *et al.* reported that the rate of carbonylation of the Pd–Me bond in several palladium–diphosphine complexes [(P–P)PdMe(solvent)]⁺, (P–P = diphosphine ligand, solvent = solvent) is at least 10 times higher than those of the corresponding neutral chloride complexes,⁵² and Liu *et al.*^{50,51,53} have recently shown that the presence of a strongly coordinating ligand such as chloride at the metal centre can have a profound effect on the individual reaction steps in the hydroalkoxycarbonylation of alkenes catalysed by Pd(II) diphosphine cations, in unfavourable cases completely inhibiting the reaction. We therefore attempted to remove the coordinated chloride from **3**(X) and replace it with a labile ligand. As noted above, coordinated chloride is not removed on addition of excess Tf(X). Addition of an excess of Ag[BF₄], to a dichloromethane–MeOH solution (8 : 1) of either **3**(Cl) or **3**[BF₄] gave several unidentified products, however, formation of Pd black was not observed. Addition of MeCN to the reaction solution resulted in an immediate colour change from orange to yellow and the formation of a new complex **5**. We have previously shown that the addition of a moderately coordinating ligand such as MeCN can stabilise the Pd(II) metal centre in analogous systems.^{50,51} The ³¹P{¹H} NMR spectrum of **5** in CH₂Cl₂–MeCN (20 : 1) solution at 193 K shows two doublets at δ (P) 41.3 and −46.3 ppm, ²J(P¹–P²) = 38.3 Hz indicative of the presence of a “chelate–monodentate” structure (Supplementary Fig. 4, ESI†). However, we have been unable to isolate **5** and

the ^1H NMR spectrum is uninformative due to exchange of solvent and coordinated MeCN. **5** is tentatively suggested to be $[\text{Pd}(\kappa^2\text{-Ph}_2\text{Ppy})(\kappa^1\text{-Ph}_2\text{Ppy})(\text{MeCN})][\text{BF}_4]_2$. Therefore, we turned our attention to other routes to halide-free chelate–monodentate complexes.

Halide-free routes to Pd(II)–Ph₂Ppy complexes

From Pd(0) precursors. Dervisi has reported that $[\text{Pd}(\kappa^1\text{-Ph}_2\text{Ppy})_2(\text{dba})]$ (**6**) is obtained on reaction of $[\text{Pd}_2(\text{dba})_3]$ with Ph₂Ppy.²⁴ Similarly, we find **6** rather than the desired “chelate–monodentate” is obtained in MeOH. Zacchini showed that on treatment with benzoquinone, in the absence of acid, dba is replaced by *p*-benzoquinone in $[\text{Pd}(\text{d}^i\text{bpx})(\text{dba})]$ ($\text{d}^i\text{bpx} = 1,2\text{-(CH}_2\text{PBU}^i_2)_2\text{C}_6\text{H}_4$),⁵⁴ in THF solution, affording $[\text{Pd}(\text{d}^i\text{bpx})(p\text{-benzoquinone})]$. We now report that treatment of $[\text{Pd}(\kappa^1\text{-Ph}_2\text{Ppy})_2(\text{dba})]$ with 1 equivalent of *p*-benzoquinone affords the new complex $[\text{Pd}(\kappa^1\text{-Ph}_2\text{Ppy})_2(p\text{-benzoquinone})]$ (**7**) in high yield as an analytically pure red solid. **7** has been characterized by an X-ray crystal structure determination. In contrast to **6**, **7** provides a convenient, halide-free route to Pd “chelate–monodentate” complexes of Ph₂Ppy.

*Crystal structure of $[\text{Pd}(\kappa^1\text{-Ph}_2\text{Ppy})_2(p\text{-benzoquinone})]$ (**7**).* Crystals of **7**, suitable for an X-ray crystal structure determination, were obtained by layering a dichloromethane solution of **7** with petroleum ether. The molecular structure of **7** is shown in Fig. 2 and selected bond lengths and angles are given in Table 3. The coordination about the metal centre is distorted square planar (if the *p*-benzoquinone ligand is considered to occupy two sites). Both of the Ph₂Ppy ligands are coordinated to palladium through phosphorus only. The average Pd–P bond lengths, 2.307 Å, are comparable to average bond lengths in the closely related complex $[\text{Pd}(\text{PPh}_3)_2(p\text{-benzoquinone})]$.⁵⁵

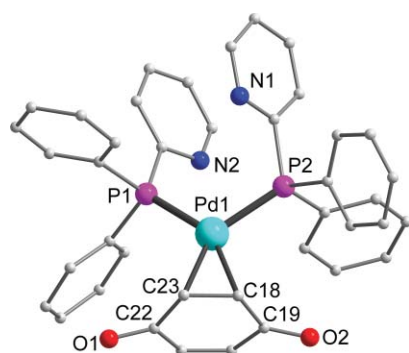


Fig. 2 The molecular structure of $[\text{Pd}(\kappa^1\text{-Ph}_2\text{Ppy})_2(p\text{-benzoquinone})]$ (**7**). H atoms removed for clarity.

Table 3 Selected bond lengths (Å) and angles (°) for $[\text{Pd}(\kappa^1\text{-Ph}_2\text{Ppy})_2(p\text{-benzoquinone})]$ (**7**)

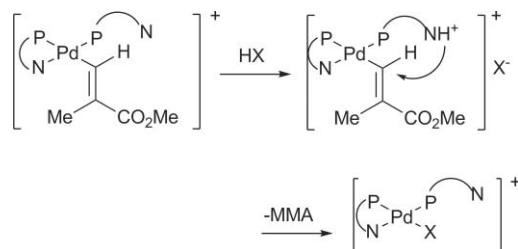
Pd–P1	2.316(2)	Pd–P2	2.299(2)
Pd–C18	2.141(6)	Pd–C23	2.187(5)
C18–C23	1.426(9)	C20–C21	1.320(9)
C19–O2	1.228(8)	C22–O1	1.233(7)
C18–Pd–C23	38.5(2)	P1–Pd–P2	105.56(5)
P1–Pd–C18	149.1(2)	P2–Pd–C23	142.4(2)

The *p*-benzoquinone molecule is κ^2 -coordinated as a mono-olefinic ligand ensuring a *cis* orientation of the $\kappa^1\text{-Ph}_2\text{Ppy}$ ligands about the metal centre. The coordinated double bond of the *p*-benzoquinone shows significant lengthening compared with the uncoordinated double bond [1.426(9) vs. 1.320(9) Å] ($\text{C}(\text{sp}^2)\text{–C}(\text{sp}^2)$ single bond range is 1.45 to 1.51 Å whereas the $\text{C}=\text{C}$ double bond of free $\text{H}_2\text{C}=\text{CH}_2$ is 1.337 Å)⁵⁵ and there is a slight twist (14.3°) in the PdP_2 to PdC_2 planes, showing this is more appropriately described as a metallacyclopropane. The twist is slightly larger (14.3 vs. 9.3°) than in the closely related complex $[\text{Pd}(\text{d}^i\text{bpx})(p\text{-benzoquinone})]$,⁵⁴ which may reflect the increased electron density at the palladium centre in the d^ibpx complex favouring metallacyclopropane formation and/or the steric constraint of the κ^2 -coordinated d^ibpx ligand compared to the less bulky Ph₂Ppy monodentate ligands of **7**. The ligand has a dihedral angle of 94.28° to the PdC_2 coordination triangle, in keeping with the κ^2 -coordination of the alkene. The steric hindrance caused by the phenyl rings forces the benzoquinone ligand to “bow”, the two $\text{C}=\text{O}$ bonds are inclined away from the metal centre, opening up the P–Pd–C angles (average 146°).

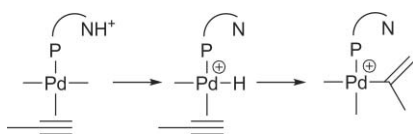
*Reactions of $[\text{Pd}(\kappa^1\text{-Ph}_2\text{Ppy})_2(p\text{-benzoquinone})]$ (**7**).* Addition of 2 equivalents of MeSO_3H to **7** results in an immediate colour change from yellow to orange. The $^{31}\text{P}\{^1\text{H}\}$ NMR spectrum reveals the presence of a new complex proposed to be $[\text{Pd}(\kappa^2\text{-Ph}_2\text{Ppy})(\kappa^1\text{-Ph}_2\text{Ppy})(\text{MeSO}_3)][\text{MeSO}_3]$ (**8** $[\text{MeSO}_3]$). **8** $[\text{MeSO}_3]$ shows resonances at $\delta(\text{P}) = 41.2$, and -40.0 ppm, $^2J(\text{P}^1\text{–P}^2) = 29.8$ Hz, indicative of the formation of a Pd(II) “chelate–monodentate” structure. Attempts to precipitate this complex as a solid were unsuccessful, impure oils being obtained (*vide infra* for further characterization of complexes of type **8**). If excess acid is used in the synthesis, a different complex $[\text{Pd}(\kappa^2\text{-Ph}_2\text{Ppy})(\kappa^1\text{-Ph}_2\text{PpyH})(\text{MeSO}_3)][\text{MeSO}_3]_2$ (**8'** $[\text{MeSO}_3]_2$), which is formed from **8** $[\text{MeSO}_3]$, is obtained. Thus, addition of 1 equivalent of MeSO_3H to a dichloromethane solution of **8** $[\text{MeSO}_3]$ under ambient conditions gives a mixture, **8** $[\text{MeSO}_3]$ and **8'** $[\text{MeSO}_3]_2$. **8'** $[\text{MeSO}_3]_2$ shows two broad resonances, at $\delta(\text{P}) = 26.0$ and -45.8 ppm in its $^{31}\text{P}\{^1\text{H}\}$ NMR spectrum, Table 1. The former resonance is in the region expected for monodentate PPh_2py , while the latter resonance shows the characteristic low frequency shift for a chelating PPh_2py ligand. The ^{31}P NMR resonances of **8'** $[\text{MeSO}_3]_2$ integrate 1:1 consistent with **8'** $[\text{MeSO}_3]$ being a Pd “chelate–monodentate” species. Both resonances show a low frequency shift compared to **8**, that of the monodentate PPh_2py ligand being particularly marked, consistent with protonation of the pyridine ring of the monodentate ligand.⁶ Addition of further aliquots of MeSO_3H results in complete conversion of **8** $[\text{MeSO}_3]$ to **8'** $[\text{MeSO}_3]_2$. Complexes with essentially identical $^{31}\text{P}\{^1\text{H}\}$ NMR spectroscopic data can be obtained by addition of 2 equivalents of Ph₂Ppy and 3 equivalents of acid to solutions of $[\text{Pd}(\text{OAc})_2]$ (Supplementary Fig. 6a, ESI†, *vide infra*). The ^1H NMR spectrum of **8'** $[\text{MeSO}_3]_2$ at 193 K shows a broad resonance at *ca.* $\delta(\text{H}) = 17.1$ ppm that integrates 1:1 against the H^6 proton of each pyridyl ring and is assigned to protonation at nitrogen.³⁴ The protons of one of the pyridyl rings also show high frequency shifts consistent with protonation of the nitrogen, for example the H^6 proton shifts from $\delta(\text{H}) = 9.17$ to 9.48 ppm (Supplementary Fig. 5b and 6b, ESI†).⁶ Scrivanti has also recently studied the protonation of pendant pyridylphosphine ligands at Pd(0) and Pd(II).⁶ We therefore decided to investigate further whether this

new complex, **8'**[MeSO₃]₂, was indeed **8**[MeSO₃] protonated at the pendant pyridyl nitrogen. Addition of 1 equivalent of MeSO₃H to a CH₂Cl₂ solution of Ph₂Ppy results in protonation at nitrogen but not phosphorus to give [Ph₂PpyH][MeSO₃]. Thus, the ¹⁵N resonance shifts to lower frequency from δ(N) = 51.2 ppm (²J(N–H) = 11 Hz and ²J(N–P) = 34 Hz) to δ(N) –168.5 ppm (²J(N–H) = 80 Hz and ²J(N–P) = 18 Hz) (Supplementary Fig. 8, ESI†). The ³¹P{¹H} NMR spectrum of [PPh₂pyH][MeSO₃], in CH₂Cl₂ at 298 K, shows a sharp singlet at δ(P) –7.8 ppm, shifted to low frequency, relative to the free ligand (δ(P) –4.5 ppm). No additional coupling on the phosphorus resonance is observed in the proton coupled ³¹P NMR spectrum, indicating protonation on the phosphorus atom has not occurred.

Protonation of the pendant pyridyl nitrogen is proposed to be an important step in the catalytic hydroesterification of alkynes using Pd/pyridylphosphine catalysts. Thus, both Drent¹⁷ and Scrivanti²⁷ report that an excess of strong acid is required to achieve high activities in the carbonylation of alkynes catalysed by Pd/PPh₂py complexes and proposed that the excess acid is required to protonate the nitrogen of a pendant pyridylphosphine ligand. Subsequent transfer of this proton to the substrate occurs either in the termination, Scheme 2, or initiation step, Scheme 3 and is proposed to account for the high activity of pyridylphosphine, compared to triarylphosphine complexes, in this catalytic system.



Scheme 2 Pyridylphosphine as a 'proton messenger' in the termination step of the methoxycarbonylation of alkynes, as proposed by Drent.

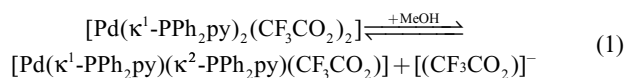


Scheme 3 Pyridylphosphine as a 'proton messenger' in the initiation step of the methoxycarbonylation of alkynes, as proposed by Scrivanti.

Preparation of chelate–monodentate complexes from Pd(II) precursors. In an attempt to obtain analytically pure complexes we have investigated the synthesis of complexes of type **8** from [Pd(OAc)₂]. Addition of two equivalents of HX, (X = OTf, MeSO₃) to a dichloromethane solution of [Pd(OAc)₂] and two equivalents of PPh₂py affords [Pd(κ²-Ph₂Ppy)(κ¹-Ph₂Ppy)(X)][X] (**8**[X]), in which one anion X is coordinated to palladium and one anion X is present as a counterion. Addition of further equivalents of HX, affords [Pd(κ²-Ph₂Ppy)(κ¹-Ph₂PpyH)(X)][X] (**8'**[X]₂). The ³¹P{¹H} NMR spectra of **8**[X] show slight variation with X, as do those of **8'**[X]₂ and are consistent with the formulations [Pd(κ²-Ph₂Ppy)(κ¹-Ph₂Ppy)(X)][X] and [Pd(κ²-Ph₂Ppy)(κ¹-Ph₂PpyH)(X)][X]₂ (Supplementary Fig. 6a, ESI†). As discussed

above, the low-frequency shift of the ³¹P{¹H} NMR resonance of the monodentate Ph₂Ppy ligand, and the appearance of a broad resonance around 17 ppm in the ¹H NMR spectra of complexes **8'** are consistent with protonation of this ligand. Addition of intermediate equivalents of acid to complexes **8** afford mixtures of **8** and **8'**, again consistent with the proposed formulations. For X = BF₄ a different complex is obtained on addition of two equivalents of HBF₄. This complex shows a single broad peak at –42.9 ppm in the ³¹P{¹H} NMR spectrum consistent with a chelating structure. Addition of further equivalents of HBF₄ converts this complex into **8'**[BF₄]₂.

We have only been able to obtain impure oils or solids of **8** and **8'** and the ¹H and ¹⁹F NMR spectra of **8**[X] and **8'**[X]₂ are uninformative regarding the ligand in the fourth coordination site at Pd due to exchange of coordinated X and the counterion, (X = OTf, MeSO₃, BF₄). However, the spectra of compounds containing the more coordinating trifluoroacetate anion are informative. Addition of CF₃COOH to a CH₂Cl₂ solution of [Pd(OAc)₂] as described above, affords a solution containing the proposed chelate–monodentate complex **8**[CF₃CO₂]. Precipitation with Et₂O affords a solid analyzing for “Pd(Ph₂Ppy)₂(CF₃CO₂)₂”. On redissolution of the solid in CH₂Cl₂, the ³¹P{¹H} NMR spectrum at 193 K (Fig. 3a) reveals the presence of two complexes, in the ratio 7 : 1, the major complex showing a broad singlet around δ(P) = 27 and the minor a pair of broad resonances at 40.8 and –38.6 ppm. This is consistent with the major compound being a bis-monodentate complex analogous to **2**, [Pd(κ¹-Ph₂Ppy)₂(CF₃CO₂)₂] ([2(CF₃CO₂)₂]) and the minor being the chelate–monodentate complex **8**[CF₃CO₂]. The ¹⁹F NMR spectrum (Fig. 3c) shows a sharp singlet at δ(F) = –75.9 consistent with the presence of a CF₃COO₂[–] counterions and a broad asymmetrical resonance which deconvolutes to minor and major resonances at δ(F) = –74.0 and –74.5, respectively, shifts consistent with coordination of CF₃COO₂[–] to Pd, *i.e.* consistent with the presence of [2(CF₃CO₂)₂] and **8**[CF₃CO₂], eqn (1), (*cf.* [Et₃NH][CF₃CO₂] δ(F) = –76.1, [Pd(OAc)₂] + CF₃CO₂H δ(F) = –74.6).



Deconvolution of the ¹⁹F NMR spectrum affords a ratio of the major complex (**2**):counterion of 7.5 : 1 consistent with the ³¹P{¹H} NMR spectroscopic data. On addition of methanol to solvate any liberated CF₃CO₂[–] ions released into solution, changes are observed in the ³¹P{¹H}, ¹⁹F, and the pyridyl region of the ¹H NMR spectra (Fig. 3, Supplementary Fig. 5b and 6b, ESI†) consistent with a change in the predominant coordination mode of the Ph₂Ppy ligands from *bis*-monodentate to chelate–monodentate. The ratio of [2(CF₃CO₂)₂] to **8**[CF₃CO₂] determined by integration of the ³¹P{¹H} NMR spectrum and by deconvolution of the ¹⁹F NMR spectrum in the presence of MeOH is 1 : 7 and 1 : 10, respectively, values in good agreement with eqn (1) within the error limits of the measurements. Taken together, these data are strongly indicative that the formulations of [2(CF₃CO₂)₂] and **8**[CF₃CO₂], and hence of **8** more generally, as [Pd(κ²-Ph₂Ppy)(κ¹-Ph₂Ppy)(X)][X] are correct. The formulation of **8'** as the protonated form of **8** is established by the ¹H and ³¹P{¹H} NMR spectra discussed above.

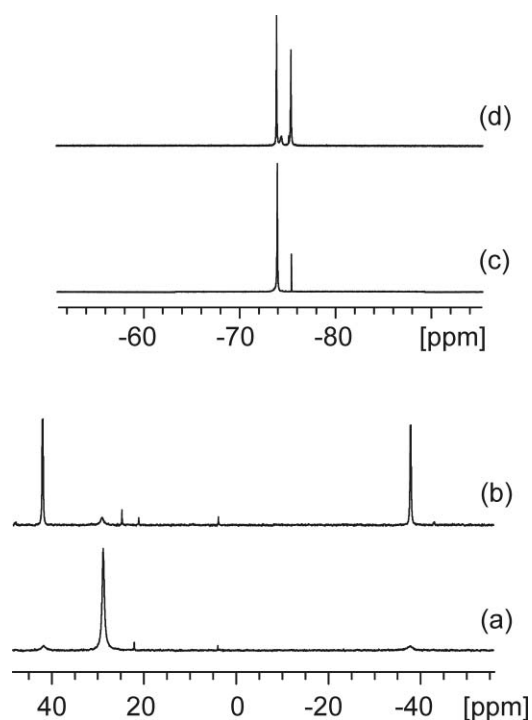


Fig. 3 NMR spectra of “Pd(Ph₂Ppy)₂(CF₃CO₂)₂” showing redistribution of the equilibrium of eqn (1) on addition of MeOH. ³¹P{¹H} NMR spectrum in (a) CH₂Cl₂ and (b) after addition of MeOH. ¹⁹F NMR spectrum in (c) CH₂Cl₂ and (d) after addition of MeOH.

Although attempts to isolate **8'** for further characterization were unsuccessful, we were successful in isolating, and characterizing, the protonated form of **2b**. Thus, addition of 2 equivalents of MeSO₃H to a dichloromethane solution of **2a/b**, results in a new complex, **2b'**, which shows a sharp singlet in the ³¹P{¹H} NMR spectrum at δ(P) = 19.1 ppm. The X-ray crystal structure of **2b'** confirms protonation occurs at the pyridyl nitrogen.

Crystal structure of trans-[Pd(κ¹-Ph₂PpyH)₂Cl₂][MeSO₃]₂ (2b'). Yellow crystals suitable for an X-ray crystal structure determination of **2b'** were obtained by layering a dichloromethane solution of **2b'** with diethyl ether. The molecular structure of **2b'** is shown in Fig. 4 and selected bond lengths and angles are given in Table 4. The coordination about the palladium centre is square planar. The Ph₂Ppy ligands are coordinated to palladium through

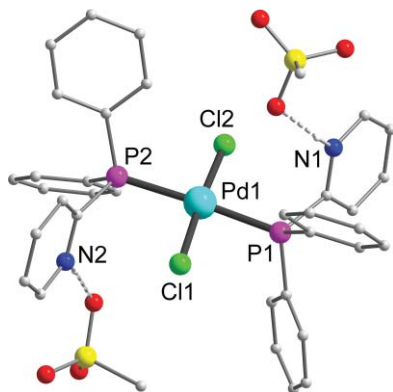


Fig. 4 Molecular structure of *trans*-[Pd(κ¹-Ph₂PpyH)₂Cl₂][MeSO₃]₂ (**2b'**), with key atoms labelled.

Table 4 Selected bond lengths (Å) and angles (°) for *trans*-[Pd(κ¹-Ph₂PpyH)₂Cl₂][MeSO₃]₂ (**2b'**)

Pd–P1	2.301(2)	Pd–Cl1	2.287(2)
Pd–P2	2.335(2)	Pd–Cl2	2.297(2)
P1–Pd–P2	176.78(6)	P1–Pd–Cl2	92.75(5)
Cl1–Pd–Cl2	175.82(5)	P2–Pd–Cl1	93.07(6)
P1–Pd–Cl1	83.83(6)	P2–Pd–Cl2	90.31(5)

phosphorus and are mutually *trans*, two terminal chloride ligands complete the coordination sphere. Both pendant nitrogen atoms of the Ph₂Ppy ligands are protonated. The average M–P bond lengths (2.317 Å) are similar to those found in **2b**. The P1–Pd–P2 and Cl1–Pd–Cl2 bond angles.

We noted above that the protonated, chelate–monodentate complex **8'**[MeSO₃]₂ can be prepared, essentially quantitatively, by addition of excess MeSO₃H to a dichloromethane solution of [Pd(OAc)₂] and PPh₂py. However, in methanol, a different complex is formed. Thus, addition of a few drops of MeSO₃H to a suspension of [Pd(OAc)₂] and 3.1 equivalents Ph₂Ppy in methanol results in immediate dissolution of the solids to give a red solution. The major species present in this solution is the previously unreported complex [Pd(κ²-Ph₂Ppy)(κ¹-Ph₂Ppy)₂][MeSO₃]₂ (**10**). Solutions of **10** are unstable giving unidentified products on standing for a few days at 293 K. On evaporation of the solvent, **10** is obtained as an impure red oil. **10** has, therefore, been formulated on the basis of its ³¹P{¹H} NMR spectrum, Fig. 5. The ¹H NMR spectra are uninformative, serving only to confirm the presence of the Ph₂Ppy ligand. At 183 K, the ³¹P{¹H} NMR spectrum of **10** shows three sets of broad resonances at δ(P) 44.7 ppm (singlet), 23.6 (doublet) and –47.7 (doublet) ppm, ²J(P²–P³) = 388 Hz, consistent with the presence of two monodentate and one chelating Ph₂Ppy ligand respectively in the complex. It is not clear from the chemical shifts of the monodentate ligands, δ(P) 44.7 and 23.6 ppm if these ligands are protonated at the pyridyl nitrogen. The low frequency shift of the latter is consistent with such protonation but may also reflect the differing *trans* ligands. In the presence of excess acid, the excess of free PPh₂py ligand is protonated at the pyridyl nitrogen, resulting in a *ca.* 1.4 ppm low frequency shift of the ³¹P NMR resonance to δ(P) –8.76 ppm.

Dynamic process in chelate–monodentate Pd(II) complexes of PPh₂py

The variable-temperature ³¹P{¹H} NMR spectra of **3**, **4**, **5**, **8'** and **10** reveal that these highly strained chelate–monodentate complexes are fluxional and we were interested to discover if this could be due to hemilability of the chelating PN ligand. Although there is evidence for dissociative processes in Pt(II) complexes,^{56–59} dissociative ligand substitution at Pd(II) is extremely uncommon,^{46,60,61} and in the presence of an incoming ligand or solvent, the alternative associative substitution is much faster. Rare examples of dissociative processes in Pd(II) complexes have been reported by Espinet.^{60,61} Although [Pd(κ²-Ph₂Ppy)(κ¹-Ph₂Ppy)₂][MeSO₃]₂ might seem an unlikely prospect for a dissociative process – it is dicationic and does not contain any electron donating organic ligands that might increase the electron density at palladium and hence enhance a dissociative pathway, the presence of the highly strained four-membered

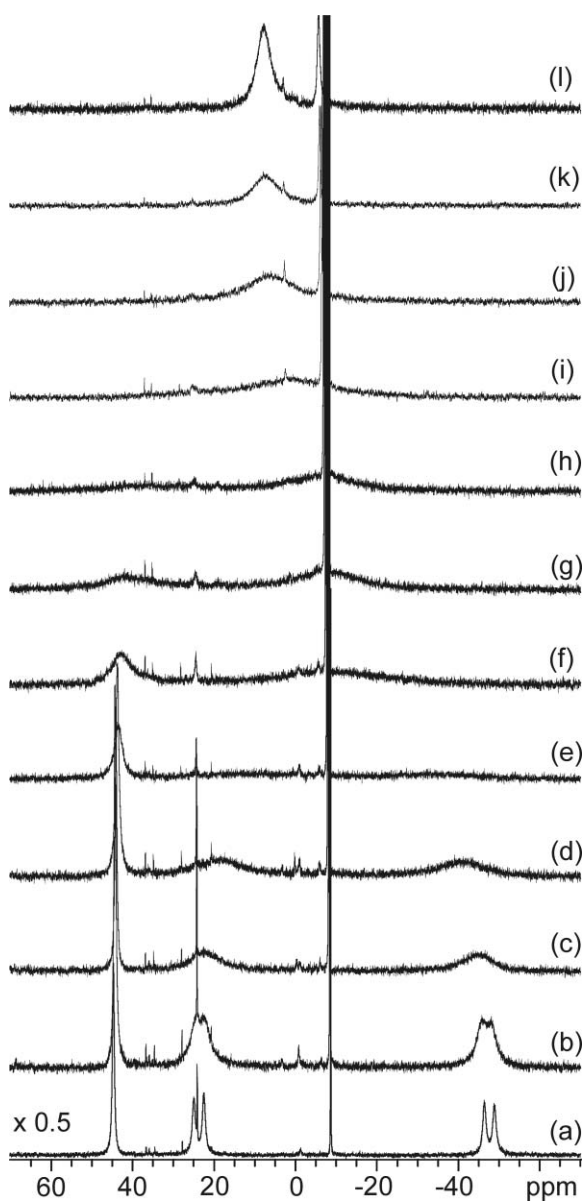
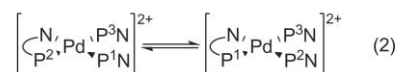
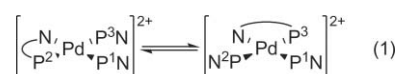


Fig. 5 $^{31}\text{P}\{^1\text{H}\}$ NMR spectrum of **10** in MeOH: (a) 183 K, (b) 193 K, (c) 203 K, (d) 213 K, (e) 223 K, (f) 233 K, (g) 243 K, (h) 253 K, (i) 263 K, (j) 273 K, (k) 283 K, (l) 293 K. The resonance at *ca.* $\delta(\text{P}) = -8.7$ ppm is due to free $[\text{PPh}_2\text{pyH}]^+[\text{MeSO}_3]^-$.

ring might, nevertheless, confer hemilability on the chelating Ph_2Ppy ligand. The fluxionality observed in **3**, **5**, and **8'** appears similar – a broadening of the resonances of the phosphorus atoms of both the chelating and monodentate ligands is observed on increasing the temperature, although the extent of broadening depends on the particular complex and counterion present.

The fluxionality observed for **4**, and **10** is more complex. For example, the NMR spectra of **10** (Fig. 5) reveal that two, stereospecific fluxional processes are occurring. The low-temperature fluxional process equivalences the chelating and monodentate 2-pyridyldiphenylphosphine ligands P^2N and P^3N (Scheme 4, eqn (1)). Such exchange has been briefly described before for $[\text{Pd}(\kappa^2\text{-Me}_2\text{Ppy})(\text{Me}_2\text{PpyX})(\text{X})]$ ($\text{X} = \text{Cl}, \text{Br}, \text{I}$), however the detailed mechanism of the exchange was not determined.³⁰ The



Scheme 4 Dynamic processes occurring in **10**.

higher temperature processes equivalences P^1N with P^2N and P^3N (Scheme 4, eqn (2)). It is not necessary that the higher energy process simultaneously equivalences all three pyridylphosphine ligands, only that it equivalences P^1N with one of P^2N or P^3N since the lower energy process already equivalences P^2N and P^3N . Since this more complex fluxional system should contain more information about the nature of the fluxional processes occurring, we began our investigations of these dynamic processes with **10**.

Dynamic process in $[\text{Pd}(\kappa^2\text{-Ph}_2\text{Ppy})(\kappa^1\text{-Ph}_2\text{Ppy})_2][\text{MeSO}_3]_2$ (**10**).

Due to its instability, solutions of **10** were prepared “*in situ*” with nominal Pd : P ratios of 1 : 3 and 1 : 3.4 and nominal Pd : MeSO_3H ratios of 1 : 2, 10, 15 or 25. This allowed the effects of excess ligand and excess acid on the fluxional processes to be investigated. We have also attempted to study the dynamic processes in CD_2Cl_2 , a non-coordinating solvent, and in mixtures of $\text{MeOH}-\text{CD}_2\text{Cl}_2$. Fig. 5 shows the variable-temperature $^{31}\text{P}\{^1\text{H}\}$ NMR spectra of **10** in the presence of a slight excess of PPh_2py (Table 5, sample 3). Two coalescence temperatures can be seen clearly, the first occurs around 223 K (Fig. 5d–f) and the second around 263 K (Fig. 5h and i). Impurities can be seen in many of the spectra (see *e.g.* Supplementary Fig. 9, *et seq.*, ESI†) of these *in situ* prepared samples. However, it should be noted that equilibrium saturation transfer difference measurements on impure **10**, in which the resonance of the chelating PPh_2py ligand at *ca.* $\delta(\text{P}) = -48$ ppm was irradiated throughout the recovery delay (3 s), revealed significant saturation transfer to the other PPh_2py ligands in **10** but *not* to those of other complexes (Supplementary Fig. 27, ESI†) indicating that the impurities do not participate in the fluxional processes. A small amount of transfer to free $[\text{PPh}_2\text{pyH}]^+$ was seen, indicating exchange with free ligand occurs, albeit slowly compared to the intramolecular exchange processes. Consistent with intermolecular exchange being slow, the resonance of $[\text{PPh}_2\text{pyH}]^+$ remains sharp until after the onset of both fluxional processes, Fig. 5 and Supplementary Fig. 19, ESI†, even when present at low concentration (Supplementary Fig. 13, 17, 21 and 23, ESI†), indicating that free $[\text{PPh}_2\text{pyH}]^+$ is not involved in these dynamic processes. The variable-temperature $^{31}\text{P}\{^1\text{H}\}$ NMR spectra have been simulated using gNMR5.1 and the activation parameters obtained, Table 5, which also gives the reaction rate constants at 213 and 243 K for the low- and high-temperature processes respectively. The spectra, spectral simulations, Eyring and Arrhenius plots are given in ESI† (Supplementary Fig. 9–26).

The reaction rate constants of the low- and high-temperature processes differ by an order of magnitude, confirming that two independent processes occur. Activation entropies in all samples are negative, consistent with an associative process, however, caution must be exercised when interpreting the data since *e.g.* changes in solvation might also contribute to the activation entropy.^{46,60,62} However, such effects are likely to be minimized in **10** since the potential dissociating ligand, the pyridyl group, is not

Table 5 Activation parameters ($\Delta S^\ddagger/\text{J mol}^{-1} \text{K}^{-1}$, $\Delta H_1^\ddagger/\text{kJ mol}^{-1}$, $E_{\text{act}}/\text{kJ mol}^{-1}$) for the dynamic processes in **10**^a

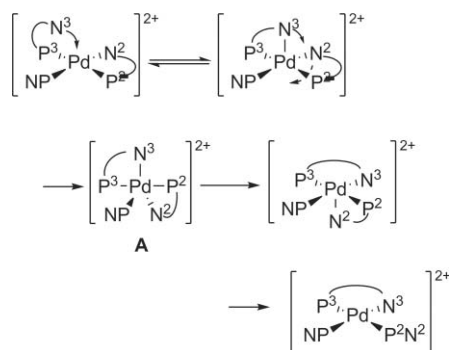
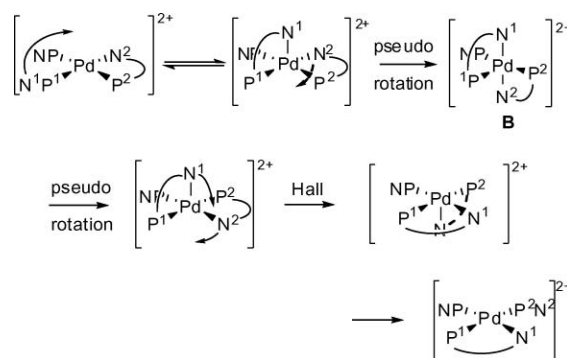
Sample	Solvent	Pd/P	Pd : MeSO ₃ H	$10^{-4}k_1^{213} b/\text{s}^{-1}$	$10^{-4}k_2^{243} b/\text{s}^{-1}$	$\Delta S_1^\ddagger c$	$\Delta S_2^\ddagger c$	$\Delta H_1^\ddagger d$	$\Delta H_2^\ddagger d$	$E_{\text{act}}^1 d$	$E_{\text{act}}^2 d$
1	MeOH	3.1	10	1.52	1.91	-15	-11	31	37	33	39
2	MeOH	3.1	10	1.23	1.37	-12	-12	32	37	34	39
3	MeOH	3.4	10	1.36	1.29	-10	-8	33	38	35	40
4	MeOH	3.4	25	1.07 ^e	1.90	-25	-33	29	39	31	41
5	MeOH	3.2	15	1.43	1.43	-25	-33	29	32	31	34
6	MeOH	2.9	25	1.11	1.16	-17	-25	31	34	34	31
7	MeOH-CD ₂ Cl ₂ (2:9)	3.1	25	8.92	1.69	-41	-32	22	32	25	34
8	MeOH-CD ₂ Cl ₂ (4:3)	3.1	5	4.11	2.13	-20	-25	24	31	28	33
9	CD ₂ Cl ₂	2.9	2	1.15 ^e	1.92 ^f	-4	-21	33	35	35	37

^a Prepared *in situ*. ^b Error $\sim \pm 10\%$. ^c Error $\sim \pm 5 \text{ J mol}^{-1} \text{K}^{-1}$. ^d Error $\sim \pm 5\%$. ^e $T = 208 \text{ K}$. ^f $T = 238 \text{ K}$.

charged. Changes in solvation are therefore expected to make only a small contribution to the activation process/parameters unless protonation–deprotonation of the pyridyl nitrogen contributes significantly.

However, the rate of the low energy process is strongly influenced by solvent, being faster in MeOH-CD₂Cl₂ mixtures than in pure MeOH. Inspection of Table 5 reveals that this rate acceleration is due to a lower enthalpy of activation, being *ca.* 23 and 33 kJ mol⁻¹, respectively (the entropy of activation is more negative in the mixed solvent). The rate of the dynamic process is marginally influenced by the presence of excess acid, compare samples 3 and 4, or with excess ligand, compare samples 1–3.

The stereoselectivity of the low-energy process is easily explained by an associative process, Scheme 5. It is reasonable to assume that the highly strained Pd(κ^2 -Ph₂Ppy) four-membered ring will prefer to adopt an axial–equatorial, rather than an equatorial–equatorial, conformation, in any intermediate/transition state of an associative process. Only two trigonal-bipyramidal intermediates are then accessible, since the law of microscopic reversibility requires that the intermediate be symmetrical (**A** and **B** in Schemes 5 and 6). **A** is directly accessible from the square-planar structure formed on chelation of the nitrogen of P³N. Movement of this nitrogen into the square plane of the complex displaces the pyridyl nitrogen of P²N, *i.e.* stereospecific equivalencing of P²N and P³N in **10** can be accomplished without movement of the phosphorus atoms following the least energetic pathway of Hall^{56,63,64} and without involving P¹N, which remains distinct. The observed solvent effect on the rate of this process might be explained by competition between methanol solvent molecules and the incoming pyridyl nitrogen for the apical coordination site.⁶⁰

**Scheme 5** Postulated intramolecular low-temperature associative mechanism in **10** following that of Hall.⁵⁶**Scheme 6** Possible intramolecular high-temperature associative mechanism in **10** involving pseudo rotations and following Hall.⁵⁶

Structure **B**, Scheme 6, which is required to equivalence P¹N by an analogous process, is not directly accessible following the least energetic pathway proposed by Hall⁵⁶ but might be obtained through a series of pseudo rotations, *cf.* the Berry pseudo rotation, Scheme 6, and will presumably, therefore, be subject to a higher activation barrier. We noted above that the rate of this process is little affected by changes in the coordinating ability of the solvent, consistent with a mechanism in which the rate determining step occurs later in the reaction coordinate. Alternative associative pathways that could account for the equivalencing of all three PPh₂py ligands in the higher energy process include a square-planar to tetrahedral reorganization of the metal centre and coordination of a fourth PPh₂py ligand to the metal centre displacing the chelating pyridyl nitrogen. The difference in activation enthalpies of the high- and low-temperature processes is rather small, *ca.* 5 kJ mol⁻¹, we therefore discount the former possibility, while the marginal effect of excess ligand on the rate would argue against the latter. Furthermore, the observed broadening of the ³¹P{¹H} NMR resonance due to PPh₂py, which is present in slight excess, is small, contrary to the differential broadening that might be expected. Thus, although the data do not exclude coordination of a fourth PPh₂py ligand as the pathway of the higher temperature process, we favour the intramolecular process shown in Scheme 6.

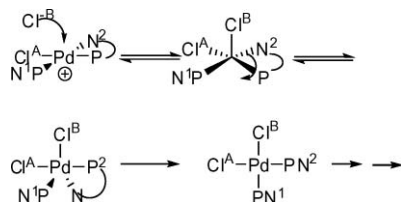
Finally, the stereospecificities observed could also be explained by a dissociative process giving a T-shaped “three-coordinate” solvated intermediate, which might occur in **10** due to the presence of the highly strained Pd(κ^2 -Ph₂Ppy) ring. Equivalencing of the *trans* disposed ligands, P²N and P³N, is then readily envisioned. However, Y-shaped structures, which have previously been proposed as high energy transition states, are necessary to interconvert

these ligands with P¹N.⁶⁵ Although, there is a recent report of T-shaped Pd(II) complexes incorporating extremely bulky phosphine ligands in which the vacant fourth coordination site is stabilized by an agostic interaction,⁶⁶ a dissociative pathway is not consistent with the negative entropy of activation and low activation barriers observed.

Dynamic process in [Pd(κ²-Ph₂Ppy)(κ¹-Ph₂Ppy)Cl]X (3(X)).

The ³¹P{¹H} NMR chemical shifts and coupling constant in 3(Cl), 3[OTf], and 3[BF₄] are essentially the same, as is expected since only the counterion has changed.^{29,30} However, the ³¹P{¹H} NMR spectrum of 3[BF₄] is sharp over the temperature range 298–193 K whilst that of 3(Cl) is significantly broadened at 293 K with the spectra of 3[OTf] showing intermediate behaviour (Supplementary Fig. 2 and 28–31, ESI†), indicating the onset of a fluxional process that is strongly influenced by the counterion. As expected for a second-order process, the rate of the fluxional process is, qualitatively, found to be concentration dependent. Analysis of second-order exchanges processes by NMR is difficult and the exchange process in 3 is sufficiently slow over the accessible temperature range that factors other than exchange make a significant contribution to the linewidth, resulting in large errors in the activation parameters that might otherwise be obtained. We therefore restrict ourselves to a qualitative discussion of the exchange process in 3.

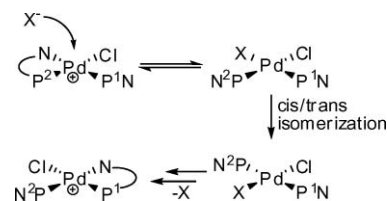
Exchange in 3[OTf] is at least an order of magnitude slower than in 3(Cl) and increasing the methanol content of the solvent mixture significantly depresses the rate. This solvent effect is consistent with a dissociative process, however, suppression of the rate by a coordinating solvent can also occur in an intermolecular associative process since competition between the incoming ligand and solvent for the fifth metal coordination site can occur.⁶⁷ Moreover, solvation of liberated Cl⁻ might be expected to be enhanced by an increase in methanol content of the solvent mixture, which would be expected to result in an increase in rate with increasing methanol content, contrary to the experimental observation. Finally, if dissociation of Cl⁻ from Pd is rate determining, then the influence of the counterion on the rate is hard to explain. Therefore, we propose that the exchange is associative and involves recoordination of the anion, Scheme 7. This is consistent with the rate suppression by MeOH, and the influence of the counterion; chloride is a “better” ligand for Pd(II) than triflate or tetrafluoroborate,⁵¹ so might be expected to re-coordinate more readily.



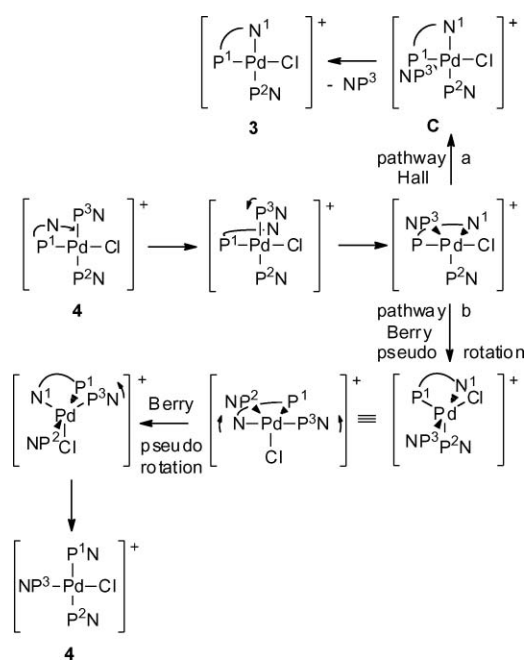
Scheme 7 Proposed mechanism to equivalence the PN ligands in 3(Cl) via recoordination of halide.

Although Scheme 7 can explain the equivalencing of the PN ligands in 3(Cl), it does not explain the equivalencing in 3[OTf], since the ligands remain distinct in the transition state, one being *trans* to ligated chloride, the other *trans* to ligated triflate.

Equivalencing of the PPh₂py ligands might be achieved by a *cis-trans* isomerization at Pd in the transition state/intermediate, Scheme 8, or via a sequence of Berry pseudo-rotations, *cf.* Scheme 9.



Scheme 8 Proposed fluxional pathway in 3[OTf].



Scheme 9 Proposed dynamic fluxional pathways in 4 starting with coordination of N¹.

Dynamic process in [Pd(κ¹-Ph₂Ppy)₃Cl](X) (4(X)). Several dynamic processes can be detected in the ³¹P{¹H} NMR spectra of 4(Cl) and 4[OTf] (Supplementary Fig. 32–40, ESI†). At temperatures below 233 K a very low energy process is seen that desymmetrizes the molecule; the *trans*-PPh₂py ligands become inequivalent. The extremely broad nature of the resonances at 193 K has prevented a detailed analysis of the dynamic process(es) involved, however, the resonance of free Ph₂Ppy is sharp at both 213 and 193 K (Supplementary Fig. 33 and 34, ESI†) indicating the low-temperature dynamic process is unlikely to involve free Ph₂Ppy. At 193 K the resonances in the aromatic region of the ¹H NMR spectrum of 4 are also extremely broad. In the solid state, π-stacking interactions are seen between the aromatic rings of P¹ and P³ and between P² and P³ and CH⋯N interactions are present between the pyridyl nitrogens of P¹ and P² and a phenyl C–H of P³, Fig. 6, inequivalencing P¹ and P². Such π-stacking may be responsible for the very low temperature dynamic process seen in the ³¹P{¹H} NMR spectra of 4.

At higher temperatures, equivalencing of all three coordinated PPh₂py ligands is seen (Supplementary Fig. 33–40, ESI†).

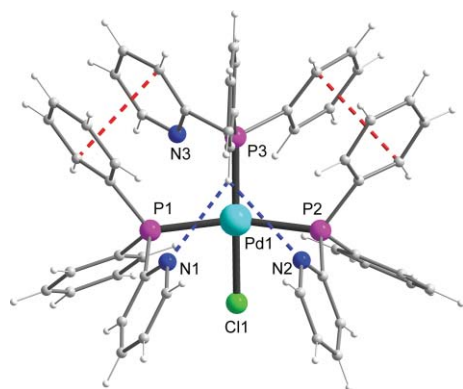
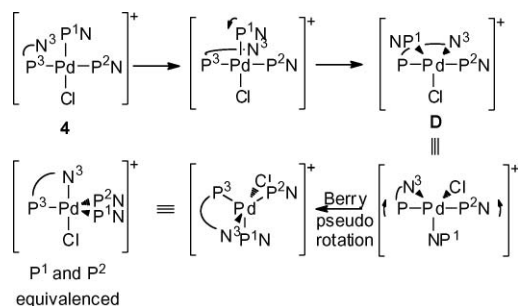


Fig. 6 Crystal structure of the monocationic complex of **4** highlighting the CH...N (blue) and π -stacking interactions (red) between the phosphine ligands.

Simulations confirm that the resonance of the pair of equivalent PPh₂py ligands broadens *faster* than that of the unique PPh₂py ligand, contrary to the expectation for a simple *intramolecular* exchange of P¹N with P^{2/3}N; *regioselective intermolecular* exchange processes must also be occurring. However, although the resonances of free PPh₂py and of traces of **3** are seen to broaden at each temperature, the spectral lineshapes of the resonances of the PPh₂py ligands in **4** are very similar, regardless of the presence or absence of free PPh₂py or **3**, or when there is a deficiency of PPh₂py, or when the counterion present is changed, compare Supplementary Fig. 33–40, ESI†. These observations indicate that the rate determining step in the equivalencing of the PPh₂py ligands in **4** is an intramolecular process. We can then suggest two scenarios for the dynamic processes in **4**: in the first, rate determining co-ordination of the pyridyl nitrogen of P¹N displaces either P²N or P³N, Scheme 9, pathway a (P³N is shown). The PPh₂py liberated is then scrambled with any free phosphine present. This process involves coordination of the nitrogen of the unique PPh₂py ligand to the apical site at Pd. Movement of one of the *trans* PPh₂py ligands, which should be kinetically favoured over that *trans* to Cl, gives a trigonal-bipyramidal intermediate **C** and ultimately gives **3**, in which the P donor atoms P¹ and P² are *cis*. By contrast, in Scheme 10, which begins with coordination of the pyridyl nitrogen of either P²N or P³N (P³N is shown) the chelate ring tethers P³ hindering displacement of P² if the Hall pathway is followed. Thus, movement of P¹N, giving species **D**, is favoured. Loss of P¹N from **D** would afford a chelate–monodentate species in which the P donors of the chelating (P³) and monodentate (P²)



Scheme 10 Proposed intramolecular fluxional pathway in **4** starting with coordination of N² or N³.

ligands are *trans* to each other, a geometry we do not observe in all other “monodentate–chelate” complexes reported here. The observed regioselectivity in exchange with free PPh₂py can thus be readily accounted for. However, the rapid equivalencing of P¹ with P^{2/3} is not accounted for by pathway a of Scheme 9 since P¹ remains *trans* to Cl.

Compare now Scheme 9 pathway b and Scheme 10. In Scheme 9, coordination of the pyridyl nitrogen of P¹ is followed by two Berry pseudo-rotations leading ultimately to equivalencing of P¹N and P³N. However, this scheme violates the principle of microscopic reversibility; the forward reaction starts with coordination of the nitrogen of the unique PPh₂py ligand, whereas the reverse reaction begins with coordination of the nitrogen of one of the pair of equivalent PPh₂py ligands. In Scheme 10, however, the reaction passes through a symmetrical intermediate/transition state as required by the principle of microscopic reversibility. Thus, coordination of the pyridyl nitrogen of P¹N accounts for regioselective exchange of P^{2/3}N with free PPh₂py (Scheme 9, pathway a) whilst coordination of the pyridyl nitrogen of P^{2/3}N accounts for equivalencing of P^{2/3}N and P¹N, Scheme 10. If the rate determining step in both processes is coordination of the pyridyl nitrogen (or loss of P³N from **D** in the *intermolecular* process), then the relative insensitivity of the rate to free phosphine and the counterion is also explained.

Simulation of the variable-temperature ³¹P{¹H} NMR spectra of **4** is complicated since more than one dynamic process is occurring over the temperature range studied and by the observation that the position of equilibrium between **3** and **4** is temperature dependent, the amount of **3** present increasing with temperature. This results in a significant low frequency shift of the coalesced resonance at higher temperature, see Supplementary Fig. 32, ESI†. It is not possible accurately to separate the variables of temperature effect on the chemical shift, concentration of **3** and the three exchange rates. Above 273 K, the simulations become less reliable due to the increasing amount of **3** present. Despite the complexity of this system we have attempted to simulate the variable-temperature spectra of solutions of **4** containing excess PPh₂py, which should displace the equilibrium between **3** + PPh₂py and **4** in favour of **4** (Supplementary Fig. 41 and 42, ESI†). The values obtained from these simulations have also been used to simulate the spectra of a sample containing stoichiometric PPh₂py (Supplementary Fig. 43, ESI†). As expected for associative processes involving rate determining intramolecular coordination of a pyridyl nitrogen, a slight suppression of rate by free PPh₂py is observed (Supplementary Table 1, ESI†) and can be attributed to competition for the apical site at Pd. Although the values obtained for ΔS^\ddagger and ΔH^\ddagger (Supplementary Table 1, ESI†) can only be regarded as approximate, we note that ΔS^\ddagger for both processes is negative, average $\Delta S_{\text{intra}}^\ddagger = -22 \text{ J mol}^{-1} \text{ K}^{-1}$, $\Delta S_{\text{inter}}^\ddagger = -19 \text{ J mol}^{-1} \text{ K}^{-1}$ similar to the values obtained for **10** and as expected for an associative process. Enthalpies of activation are also similar to those for **10**, again consistent with rate determining association of a pyridyl nitrogen.

Conclusions

Pd-PPh₂py chelate complexes have been suggested as intermediates in palladium-catalysed alkoxy-carbonylation of propyne. However, prior to the work presented here, the preferred

coordination mode of Ph₂Ppy to Pd(II) was, almost universally, found to be monodentate coordination through phosphorus. In contrast to these earlier reports, the present work has shown that stable chelating palladium(II) complexes of Ph₂Ppy are readily prepared by the use of solvent systems such as MeOH or CH₂Cl₂–MeOH, in which MeOH presumably solvates the counterion. Protonation of the pyridyl nitrogen of monodentate coordinated PN in these complexes by the strong acid present in such alkyne methoxycarbonylation catalyst systems as proposed by Drent,^{7,17} Tooze,²⁵ Scrivanti,^{6,27} and Elsevier,²² is observed. However, in the solvent systems used (*i.e.* MeOH) we have shown that such protonation does not preclude the formation of κ²-PPh₂py complexes.

The presence of severe strain in the Pd(κ²-PPh₂py) ring in ‘chelate–monodentate’ complexes might suggest Ph₂Ppy could act as a hemilabile ligand furnishing a vacant coordination site through de-coordination and re-coordination of the pyridyl nitrogen: variable-temperature ³¹P{¹H} NMR spectroscopy reveals that dynamic processes do occur in Pd(κ²-PPh₂py). For example, two stereospecific exchanges occur in **10**, the lower energy process equivalences the *trans* disposed ligands P²N and P³N, while a higher energy process equivalences all three PN ligands (Schemes 5 and 6). Both mechanisms have a negative entropy of activation consistent with an associative intramolecular exchange pathway. Similarly, the dynamic processes in **4** can be explained by rate determining coordination of a pyridyl nitrogen to palladium. The dynamic exchange process observed in **3** is also probably associative but involves re-coordination of the counterion displacing the chelating nitrogen. Thus, although “Pd(κ²-PPh₂py)” complexes may well be present in catalyst systems using Ph₂Ppy as a ligand, it is not certain that the catalytic reaction will proceed *via* ligand hemilability. Indeed, when weakly coordinating ligands, such as methanesulfonate are present, it is these, and not the nitrogen of the chelating Ph₂Ppy ligand, which are the more labile despite the strain in the chelate ring.

Experimental

General methods and procedures

All manipulations involving solutions or solids were performed under an atmosphere of nitrogen using standard Schlenk techniques. All solvents were dried and distilled under nitrogen following standard literature methods; *i.e.* CH₂Cl₂ over CaH₂, MeOH over Mg(OMe)₂, EtOH over Mg, THF over Na/benzophenone, MeCN over CaH₂, *n*-hexane over Na and Et₂O over Na/benzophenone. Deuterated solvents were degassed by three freeze–pump–thaw cycles under vacuum in a liquid-nitrogen bath, then nitrogen saturated and stored over activated 4 Å molecular sieves under nitrogen for at least 24 h prior to use. Some compounds were obtained as impure oils and have been characterized in solution only by NMR spectroscopy. No yield or elemental analysis is reported for these compounds. Reactions involving CO were carried out in a well ventilated fume-hood. All other experiments have been carried out following standard safety procedures.

³¹P{¹H}, ³¹P, ¹³C{¹H}, ¹³C and ¹H NMR measurements were performed on Bruker AMX2-200WB, AMX400, DPX400 or Avance2-400 instruments using commercial probes. Chemical

shifts were referenced to TMS following IUPAC guidelines. Spectra of samples dissolved in non-deuterated solvents were referenced *via* the solvent resonances. Chemical shift errors are as follows; ³¹P ± 0.2 ppm, ¹H ± 0.05 ppm. Coupling constant errors are as follows; ³¹P ± 1.0 Hz, ¹H ± 0.1 Hz. In reporting NMR data the letters s, d, t *etc.* have their normal meaning. Mass spectrometric analyses were run in ES+ (positive electrospray) ionisation mode on a Micromass LCT instrument using a ‘Time of Flight’ mass analyser. X-Ray structures were determined on a Bruker Smart APEX CCD diffractometer at 100 K using graphite monochromated Mo-Kα radiation (λ = 0.71073 Å). Crystals were coated with nujol and then mounted on a glass fibre. Structures were solved by direct methods and structure refinements by full-matrix least-squares were based on all data using *F*². All non-hydrogen atoms were refined anisotropically unless otherwise stated. Hydrogen positions were placed geometrically. Microanalyses were performed at the University of Liverpool using a Leeman CE440 CHN Analyser or by Butterworth Laboratories Ltd.

All chemical reagents were purchased from Aldrich Chemical Co., except [Pd₂dba₃],⁶⁸ [Pd(Ph₂CN)₂Cl₂]⁶⁹ and [Pd(Ph₂Ppy)₂dba]²⁴ which were prepared by published methods. ¹³CO (99.98%) was purchased from Isotec Inc.

[Pd(κ²-Ph₂Ppy)Cl₂] (1). Ph₂Ppy (0.037 g, 0.14 mmol) was added to a solution of [Pd(PhCN)₂Cl₂] (0.054 g, 0.14 mmol) in dichloromethane (10 mL) and the mixture stirred for 30 min. The resultant yellow solution was reduced to half volume *in vacuo* and diethyl ether was added to precipitate an impure yellow solid. The yellow solid, comprising a mixture of **1** with **2a/b** from which pure **1** could not be isolated, was filtered through a sinter, washed with diethyl ether (3 × 20 mL) and dried *in vacuo* to afford 0.054 g of the solid mixture. ³¹P{¹H} NMR in CH₂Cl₂: δ(P) –61.6 (s, **1**); 29.0 (s, **2a**); 22.8 (s, **2b**).

[Pd(κ¹-Ph₂Ppy)₂Cl₂] (2a/b). Ph₂Ppy (0.308 g, 1.17 mmol) was added to a solution of [Pd(COD)Cl₂] (0.157 g, 0.56 mmol) in dichloromethane (10 mL) and the mixture stirred for 30 min. The resultant yellow solution was reduced to half volume *in vacuo* and diethyl ether was added to precipitate the product as a yellow solid. The yellow solid was filtered through a sinter, washed with diethyl ether (3 × 20 mL) and dried *in vacuo*. Yield: 0.358 g, 91%. Anal. Calc. for C₃₄H₂₈N₂P₂Cl₂Pd: C, 58.02; H, 4.01; N, 3.98. Found: C, 57.82; H, 4.02; N, 3.82%. MS (ES⁺, *m/z*): 667, [M – Cl]⁺. ³¹P{¹H} NMR in CH₂Cl₂: δ(P) 29.0 (s, **2a**); 22.8 (s, **2b**).

trans-[Pd(κ¹-Ph₂Ppy)₂Cl₂] (2b). A dichloromethane solution of **2a/b** was layered with diethyl ether. Crystals suitable for an X-ray crystal structure determination were obtained upon slow diffusion of the layers. Upon redissolution of the crystals in CH₂Cl₂, the ³¹P{¹H} NMR showed a mixture of *cis* and *trans* isomers was present.

[Pd(κ²-Ph₂Ppy)(κ¹-Ph₂Ppy)Cl]Cl (3(Cl)). A few drops of MeOH were added to a suspension of **2a/b** (0.025 g, 0.036 mmol) in dichloromethane (2 mL) and the mixture shaken for a few minutes until a clear yellow solution was obtained. Solvent was removed *in vacuo* to give a yellow powder. Yield: 0.0238 g, 95%. Anal. Calc. for C₃₄H₂₈N₂P₂Cl₂Pd: C, 58.02; H, 4.01; N, 3.98; Cl, 10.07. Found: C, 57.59; H, 3.98; N, 3.69; Cl, 10.33%. MS (ES⁺, *m/z*): 667, [M]⁺. NMR in CH₂Cl₂–MeOH at 233 K: δ(H) 8.77 (br, 1H, Ph₂Ppy, H⁶-py), 8.12 (br, 1H, *J*(HH) ~ 7 Hz, Ph₂Ppy,

H⁴-py), 7.9–7.3 (24H, Ph₂Ppy); $\delta(P)$ 44.4 (d, $^2J(P^1-P^2) = 33.0$ Hz, κ^1 -Ph₂Ppy), –44.0 (d, κ^2 -Ph₂Ppy).

[Pd(κ^2 -Ph₂Ppy)(κ^1 -Ph₂Ppy)Cl][BF₄] (3[BF₄]). Ag[BF₄] (0.182 g, 0.93 mmol) was added to a suspension of **2a/b** (0.657 g, 0.93 mmol) in methanol–dichloromethane (1 : 1, 20 mL) and the resultant red mixture stirred for 1 h. AgCl was removed by filtration through Celite and the resultant clear solution reduced to *ca.* 5 mL *in vacuo*. MeOH (15 mL) was added to induce precipitation of 3[BF₄] as yellow crystals which were suitable for an X-ray crystal structure determination. Yield: 0.536 g, 76%.

Alternative procedure. Dichloromethane (2 mL) was added to a solid mixture of Ti[BF₄] (0.029 g, 0.1 mmol) and **2a/b** (0.070 g, 0.1 mmol). The resulting solution was stirred for 1 h then filtered from the precipitate of TiCl into 25 mL of Et₂O. The resulting precipitate was washed three times with Et₂O by decantation, collected by filtration and dried *in vacuo*. Anal. Calc. for C₃₄H₂₈N₂P₂ClBF₄Pd: C, 54.07; H, 3.74; N, 3.71. Found: C, 53.88; H, 3.63; N, 3.66%. MS (ES⁺, *m/z*): 667, [M⁺]. NMR in CH₂Cl₂–MeOH at 233 K: $\delta(H)$ 8.77 (br, 1H, Ph₂Ppy, H⁶-py), 8.12 (t, 1H, *J*(HH) ~ 7 Hz, Ph₂Ppy, H⁴-py), 7.9–7.3 (24H, Ph₂Ppy); $\delta(P)$ 44.8 (d, κ^1 -Ph₂Ppy), –43.8 (d, $^2J(P^1-P^2) = 38.2$ Hz, κ^2 -Ph₂Ppy); $\delta(F)$ –152.5.

[Pd(κ^2 -Ph₂Ppy)(κ^1 -Ph₂Ppy)Cl][MeSO₃] (3[MeSO₃]). Dichloromethane (2 mL) was added to a solid mixture of Ti[MeSO₃] (0.035 g, 0.1 mmol) and **2a/b** (0.070 g, 0.1 mmol). The resulting solution was stirred for 1 h then filtered from the precipitate of TiCl into 25 mL of Et₂O. The resulting precipitate was washed three times with Et₂O by decantation, collected by filtration and dried *in vacuo*. NMR in CH₂Cl₂–MeOH at 233 K: $\delta(H)$ 8.77 (br, 1H, Ph₂Ppy, H⁶-py), 8.12 (t, br, 1H, *J*(HH) ~ 7 Hz, Ph₂Ppy, H⁴-py), 7.9–7.3 (24H, Ph₂Ppy); $\delta(P)$ 44.7 (d, $^2J(P^1-P^2) = 38.2$ Hz, κ^1 -Ph₂Ppy), –43.8 (d, κ^2 -Ph₂Ppy). $\delta(^{19}F)$ –153.03 ppm. MS (ES⁺, *m/z*): 667, [M⁺].

[Pd(κ^2 -Ph₂Ppy)(κ^1 -Ph₂Ppy)Cl][OTf] (3[OTf]). Dichloromethane (2 mL) was added to a solid mixture of Ti[OTf] (0.035 g, 0.1 mmol) and **2a/b** (0.070 g, 0.1 mmol). The resulting solution was stirred for 1 h then filtered from the precipitate of TiCl into 25 mL of Et₂O. The resulting precipitate was washed three times with Et₂O by decantation, collected by filtration and dried *in vacuo*. Anal. Calc. for C₃₃H₂₈ClF₃N₂O₃P₂PdS·0.5CD₂Cl₂: C, 49.52; H, 3.51; N, 3.25. Found: C, 49.32; H/D, 3.40; N, 3.25%. NMR in CH₂Cl₂–MeOH at 233 K: $\delta(H)$ 8.77 (br, 1H, Ph₂Ppy, H⁶-py), 8.12 (t, 1H, *J*(HH) ~ 7 Hz, Ph₂Ppy, H⁴-py), 7.9–7.3 (24H, Ph₂Ppy); $\delta(P)$ 44.6 (d, $^2J(P^1-P^2) = 38.1$ Hz, κ^1 -Ph₂Ppy), –43.9 (d, κ^2 -Ph₂Ppy). MS (ES⁺, *m/z*): 667, [M⁺].

[Pd(κ^1 -Ph₂Ppy)₃Cl](Cl) (4(Cl)). Ph₂Ppy (0.058 g, 0.22 mmol) was added to a solution of [Pd(κ^2 -Ph₂Ppy)(κ^1 -Ph₂Ppy)Cl]Cl, 3(Cl), (0.156 g, 0.22 mmol) in dichloromethane–MeOH (1 : 1) (20 mL) and stirred for 1 h. The resultant yellow solution was reduced to *ca.* 1 mL *in vacuo*. Crystals of 4(Cl) suitable for an X-ray crystal structure determination were obtained by slow removal of solvent from a saturated dichloromethane–MeOH solution at reduced pressure. NMR in CD₂Cl₂ at 293 K: $\delta(H)$ 8.39 (br) (3H, Ph₂Ppy, H⁶-py), 7.22 (br t, 3H, *J*(HH) ~ 5.4 Hz, Ph₂Ppy, H-py), 7.11 (dd, br, 3H, *J*(HH) ~ 7.25 Hz, Ph₂Ppy, H-py), 7.57–7.29 (30H, Ph₂Ppy). At 233 K: $\delta(P)$ 33.1 (br, κ^1 -Ph₂Ppy), 25.7 (br, κ^2 -Ph₂Ppy)

[Pd(κ^1 -Ph₂Ppy)₃Cl][OTf] (4[OTf]). Dichloromethane–MeOH (1 : 1) (2 mL) was added to a solid mixture of Ph₂Ppy (0.022 g, 0.084 mmol) and [Pd(κ^2 -Ph₂Ppy)(κ^1 -Ph₂Ppy)Cl]Cl, 3(Cl), (0.051 g, 0.068 mmol). Ti[OTf] (0.025 g, 0.071 mmol) was added to the solution and the mixture stirred for 1 h. The resultant colourless solution was filtered from the precipitate of TiCl into 5 mL of Et₂O. The resulting precipitate was washed three times with Et₂O by decantation, collected by filtration and dried *in vacuo*. The precipitate analyzes as 4[OTf]·CD₂Cl₂. Yield 0.068 g, 80%. Anal. Calc. for C₃₃H₄₂D₂Cl₃F₃N₃O₃P₃PdS: C, 54.51; H/D, 3.97; N, 3.60. Found: C, 54.69; H/D, 3.83; N, 3.80%. MS (ES⁺, *m/z*): 667, [M⁺ – PPh₂(C₅H₃N)]. NMR in CD₂Cl₂ at 293 K: $\delta(H)$ 8.39 (br, 3H, Ph₂Ppy, H⁶-py), 7.22 (t, br, 3H, *J*(HH) ~ 5.4 Hz, Ph₂Ppy, H-py), 7.11 (dd, br, 3H, *J*(HH) ~ 7.25 Hz, Ph₂Ppy, H-py), 7.57–7.29 (30H, Ph₂Ppy). NMR in CD₂Cl₂ at 233 K: $\delta(H)$ 8.33 (br, 1H, Ph₂Ppy, H⁶-py), 8.29 (br, 2H, Ph₂Ppy, H⁶-py), 7.84–7.26 (29H, Ph₂Ppy), 7.22 (t, br, 2H, Ph₂Ppy, H-py), 7.17 (br, 1H, Ph₂Ppy, H-py), 7.11 (br, 1H, Ph₂Ppy, H-py), 7.00 (d, br, 2H, Ph₂Ppy, H-py), 6.25 (br, 1H, Ph₂Ppy, H-py); $\delta(P)$ 33.2 (br, κ^1 -Ph₂Ppy), 25.6 (br, κ^2 -Ph₂Ppy)

[Pd(κ^2 -Ph₂Ppy)(κ^1 -Ph₂Ppy)(MeCN)][BF₄] (5). Excess Ag[BF₄] (0.131 g, 0.67 mmol) was added to a solution of 3(Cl) (0.225 g, 0.32 mmol) in a 1 : 1 dichloromethane–MeOH (20 mL), and MeCN was added (1 mL). The mixture was stirred in the dark for 2 h, then filtered through celite to remove AgCl and unreacted Ag[BF₄]. The resultant yellow solution was reduced to *ca.* 2 mL *in vacuo* and diethyl ether added to precipitate the complex as a yellow oil. NMR in CH₂Cl₂ at 193 K: $\delta(P)$ 41.3 (d, $^2J(PP) = 38.3$ Hz, κ^1 -Ph₂Ppy), –46.3 (d, κ^2 -Ph₂Ppy).

[Pd(κ^1 -Ph₂Ppy)₂(*p*-benzoquinone)] (7). Dichloromethane (20 mL) was added to a solid mixture of [Pd(dba)₂] (1.00 g, 1.74 mmol), 2-pyridyldiphenylphosphine (0.98 g, 3.72 mmol) and *p*-benzoquinone (0.188 g, 1.74 mmol) and the mixture stirred under N₂ for 3 h. The resultant red solution was filtered and the filtrate concentrated to *ca.* 2 mL. Petroleum ether (15 mL) was then added to precipitate the product as a red powder. The powder was collected by filtration, washed with petroleum ether (3 × 20 mL) and dried *in vacuo*. Yield: 0.54 g, 79%. Crystals suitable for X-ray structure determination were obtained by slow diffusion of petroleum ether into a dichloromethane solution of 7 (0.05 g, 0.067 mmol). Anal. Calc. for C₄₀H₃₂N₂O₂P₂Pd: C, 64.83; H, 4.35; N, 3.78. Found: C, 64.67; H, 4.24; N, 3.52%. NMR in CH₂Cl₂ at 293 K: $\delta(P)$ 30.2 (s).

[Pd(κ^2 -Ph₂Ppy)(κ^1 -Ph₂Ppy)(MeSO₃)] [MeSO₃] (8(MeSO₃)). MeSO₃H (14.4 μ L, 0.22 mmol) was added to a solution of 7 (0.082 g, 0.11 mmol) in dichloromethane (2 mL) to give a yellow–orange solution. Attempts to isolate 8 by solvent removal *in vacuo* resulted in the formation of a yellow oil.

[Pd(κ^2 -Ph₂Ppy)(κ^1 -Ph₂Ppy)X][X] (8[X]). (X = MeSO₃, OTf, CF₃CO₂). MeSO₃H (13 μ L, 0.20 mmol) was added to a solution of [Pd(OAc)₂] (0.022 g, 0.1 mmol) and Ph₂Ppy (0.053 g, 0.2 mmol) in dichloromethane (2 mL) to give a yellow–orange solution, which was stirred for 1 h, then filtered by cannula into 25 mL of Et₂O. The resulting precipitate was washed three times with Et₂O by decantation, collected by filtration and dried *in vacuo*. The triflate and trifluoroacetate complexes were prepared analogously.

8[MeSO₃]: NMR in CH₂Cl₂ at 193 K: $\delta(H)$ 9.17 (br, 1H, Ph₂Ppy, H⁶-py), 8.25 (t, br, 1H, *J*(HH) ~ 7 Hz, Ph₂Ppy, H⁴-py), 7.98–7.11

(24H, Ph₂Ppy); $\delta(\text{P})$ 41.2 (d, $^2J(\text{P}^1-\text{P}^2) = 29.8$ Hz, $\kappa^1\text{-Ph}_2\text{Ppy}$), -40.0 (d, $\kappa^2\text{-Ph}_2\text{Ppy}$). **8[X]** (X = OTf, CF₃CO₂) were prepared similarly.

8[OTf]: Calc. for C₃₆H₂₈F₆N₂O₆P₂PdS₂: C, 46.44; H, 3.03; N, 3.01. Found: C, 46.84; H/D, 3.40; N, 3.17%. NMR in CH₂Cl₂ at 193 K: $\delta(\text{H})$ 8.7 (br, 1H, Ph₂Ppy, H⁶-py), 8.35 (br, 1H, $J(\text{HH}) \sim 7$ Hz, Ph₂Ppy, H⁴-py), 8.07 = 7.13 (24H, Ph₂Ppy); $^{31}\text{P}\{^1\text{H}\}$ $\delta(\text{P})$ 40.8 (d, br, $\kappa^1\text{-Ph}_2\text{Ppy}$), -39.3 (d, br, $\kappa^2\text{-Ph}_2\text{Ppy}$).

8[CF₃CO₂]: NMR in CH₂Cl₂ at 193 K: $\delta(\text{H})$ 8.5 (br, 1H, Ph₂Ppy, H⁶-py), 8.25 (t, br, 1H, $J(\text{HH}) \sim 7$ Hz, Ph₂Ppy, H⁴-py), 7.9 = 7.2 (24H, Ph₂Ppy); $\delta(\text{P})$ 40.8 (d, $^2J(\text{P}^1-\text{P}^2) = 24.4$ Hz, $\kappa^1\text{-Ph}_2\text{Ppy}$), -38.6 (d, $\kappa^2\text{-Ph}_2\text{Ppy}$).

[Pd($\kappa^2\text{-Ph}_2\text{Ppy})(\kappa^1\text{-Ph}_2\text{PpyH})\text{X}](\text{X})_2$ (**8'(X)**). One equivalent of XH, (X = OTf, MeSO₃, BF₄) was added with stirring to a solution **8[X]** in a dichloromethane (2 ml) solution prepared as described above. The resulting solution was stirred for 1 h, then filtered by cannula into 10 mL of Et₂O. The resulting precipitate was washed three times with Et₂O by decantation, collected by filtration and dried *in vacuo*.

8'[OTf]: NMR in CH₂Cl₂ at 193 K: $\delta(\text{H})$ 9.31 (br, 1H, Ph₂Ppy, H⁶-py), 8.93 (br, 1H, Ph₂Ppy, H⁴-py), 8.67 (t, br, 1H, $J(\text{HH}) \sim 7$ Hz, Ph₂Ppy, H⁵-py), 8.35 (br) (1H, Ph₂Ppy, H⁴-py), 8.05–7.2 (22H, Ph₂Ppy); $\delta(\text{P})$ 26.4 (d, br, $^2J(\text{P}^1-\text{P}^2) = 8$ Hz, $\kappa^1\text{-Ph}_2\text{Ppy}$), -45.0 (d, br, $\kappa^2\text{-Ph}_2\text{Ppy}$).

8'[MeSO₃]: NMR in CH₂Cl₂ at 193 K: $\delta(\text{H})$ 9.48 (br, 1H, Ph₂Ppy, H⁶-py), 9.11 (br, 1H, Ph₂Ppy, H⁴-py), 8.61 (br, 1H, $J(\text{HH}) \sim 7$ Hz, Ph₂Ppy, H⁵-py), 8.35 (br, 2H, Ph₂Ppy, H⁴-py), 8.06–7.3 (22H, Ph₂Ppy); $\delta(\text{P})$ 26.0 (br, $\kappa^1\text{-Ph}_2\text{Ppy}$), -45.8 (br, $\kappa^2\text{-Ph}_2\text{Ppy}$).

8'[BF₄]: NMR in CH₂Cl₂ at 193 K: $\delta(\text{H})$ 9.33 (br, 1H, Ph₂Ppy, H⁶-py), 8.79 (br, 2H, Ph₂Ppy, H⁴-py), 8.5 (br, 1H, $J(\text{HH}) \sim 7$ Hz, Ph₂Ppy, H⁵-py), 8.36 (br, 1H, Ph₂Ppy, H⁴-py), 8.09–7.2 (22H, Ph₂Ppy); $\delta(\text{P})$ 25.2 ($\kappa^1\text{-Ph}_2\text{Ppy}$), -43.7 ($\kappa^2\text{-Ph}_2\text{Ppy}$).

"Pd(Ph₂Ppy)₂(CF₃CO₂)₂" (**2(CF₃CO₂)₂/8(CF₃CO₂)**). CF₃CO₂H (15 μL , 0.22 mmol) was added to a solution of palladium acetate (0.022 g, 0.1 mmol) and Ph₂Ppy (0.053 g, 0.2 mmol) in dichloromethane (2 mL) to give a yellow–orange solution. The solution was decanted into 3 mL Et₂O and the pale orange precipitate collected by filtration and dried. The precipitate analyzes as [Pd(Ph₂Ppy)₂(CF₃CO₂)₂].CH₂Cl₂. Anal. Calc. for C₃₈H₂₈Cl₂F₆N₂O₄P₂Pd: C, 49.08; H, 3.03; N, 3.01. Found: C, 48.67; H, 3.05; N, 4.02. NMR in CH₂Cl₂ at 193 K: **2(CF₃CO₂)₂**: $\delta(\text{H})$ 8.58 (2H, H⁶-py), 8.13–7.17 (26H, PPh₂py); $\delta(\text{F})$ -74.5 (br, $\kappa^1\text{-CF}_3\text{CO}_2$); $\delta(\text{P})$ 27.6 (br) ($\kappa^1\text{-Ph}_2\text{Ppy}$); **8[CF₃CO₂]**: $\delta(\text{F})$ -74.0 (br, $\kappa^1\text{-CF}_3\text{CO}_2$) -75.9 ([CF₃CO₂][−]); $\delta(\text{P})$ 40.8 (br, $\kappa^1\text{-Ph}_2\text{Ppy}$), -38.6 (br, $\kappa^2\text{-Ph}_2\text{Ppy}$). NMR in CH₂Cl₂–MeOH at 193 K: **2(CF₃CO₂)₂**: $\delta(\text{F})$ -74.5 (br) ($\kappa^1\text{-CF}_3\text{CO}_2$); $\delta(\text{P})$ 27.7 (br, $\kappa^1\text{-Ph}_2\text{Ppy}$); **8[CF₃CO₂]**: $\delta(\text{H})$ 8.49 (1H, H⁶-py), 8.25 (1H, H⁶-py), 8.13–7.17 (27H, PPh₂py); $\delta(\text{P})$ 40.8 (d, $^2J(\text{PP})$ -24.5 Hz, $\kappa^1\text{-Ph}_2\text{Ppy}$), -38.6 (d, $\kappa^2\text{-Ph}_2\text{Ppy}$); $\delta(\text{F})$ -74.0 (br, $\kappa^1\text{-CF}_3\text{CO}_2$), -75.6 ([CF₃CO₂][−]).

[Pd($\kappa^2\text{-Ph}_2\text{Ppy})_2$][BF₄]₂ (**9**). HBF₄·Et₂O (27 μL , 0.20 mmol) was added to a solution of [Pd(OAc)₂] (0.022 g, 0.1 mmol) and Ph₂Ppy (0.053 g, 0.2 mmol) in dichloromethane (2 mL) to give an immediate yellow–orange precipitate. The precipitate was collected by filtration, washed three times with Et₂O and dried *in vacuo*. The precipitate analysed as **9**·2CH₃CO₂H·H₂O.

Resonances attributable to acetic acid and water integrating as 1 : 2 : 1 (**9**: AcOH : H₂O) were observed in the ¹H NMR spectrum.

Anal. Calc. for C₃₈H₃₈B₂F₈N₂O₅P₂Pd: C, 48.31; H, 4.05; N, 2.97. Found: C, 47.39; H, 3.95; N, 3.4%. NMR in CDCl₃ at 293 K: $\delta(\text{H})$ 9–6.7 (PPh₂py, 26H), 2.51 (CH₃CO₂H + H₂O, 4H), 2.18 (CH₃CO₂H, 6H); in CH₂Cl₂ at 193 K: $\delta(\text{P})$ -42.9 (br, $\kappa^2\text{-Ph}_2\text{Ppy}$).

[Pd($\kappa^2\text{-Ph}_2\text{Ppy})(\kappa^1\text{-Ph}_2\text{Ppy})_2$][MeSO₃]₂ (**10**). Methanol (2 mL) was added to a solid mixture of [Pd(OAc)₂] (0.116 g, 0.52 mmol) and Ph₂Ppy (0.409 g, 1.55 mmol). The resultant yellow solution turned red on addition of MeSO₃H (67 μL , 1.04 mmol). A red oil was obtained upon removal of the solvent *in vacuo*. Anal. NMR in MeOH at 293 K: $\delta(\text{H})$ 8.26 (br, 3H, Ph₂Ppy, H⁶-py), 7.99 (t, br, 3H, $J(\text{HH}) \sim 5.4$ Hz, Ph₂Ppy, H-py), 7.7–7.3 (33H, Ph₂Ppy). NMR in MeOH at 183 K: $\delta(\text{H})$ 9–7 (33H, Ph₂Ppy); $\delta(\text{P})$ 44.7 (s, br, $\kappa^1\text{-Ph}_2\text{Ppy}$), 23.6 (d, br, $^2J(\text{trans-P}^2\text{-P}^3) = 388$ Hz, $\kappa^1\text{-Ph}_2\text{Ppy}$) -47.7 (d, br, $\kappa^2\text{-Ph}_2\text{Ppy}$).

Variable-temperature NMR spectroscopic measurements for 3. Typically, a 0.0178 mmol solution of **3(Cl)** in dichloromethane was used. For **3[OTf]**, one equivalent of Ag[OTf] was added to the solution, and the supernatant liquid decanted from the AgCl precipitate before transferring the solution to an NMR tube. The variable-temperature $^{31}\text{P}\{^1\text{H}\}$ NMR spectra were recorded, and simulated using gNMR5.1.

Variable-temperature NMR spectroscopic measurements for 4. Typically, dichloromethane–MeOH (1 : 1) solutions of **4** (0.060 mmol) were prepared by addition of ~ 1 equivalent of Ph₂Ppy to **3(Cl)**. To prepare the triflate salt 1 equivalent of Ti[OTf] was added to the solution and the precipitate of TiCl removed by filtration. The variable-temperature $^{31}\text{P}\{^1\text{H}\}$ NMR spectra were recorded, and simulated using gNMR5.1.

Determination of activation parameters for 10. Typically, MeSO₃H (130 mg, 1.37 mmol) was added to a suspension of (0.015 g, 0.064 mmol) palladium acetate in methanol (0.75 mL) to give a red solution. This solution was transferred to an NMR tube and the variable-temperature $^{31}\text{P}\{^1\text{H}\}$ NMR spectra recorded, simulated using gNMR5.1 and ΔS^\ddagger , ΔH^\ddagger and E_{act} were obtained from Eyring and Arrhenius plots respectively.

Spectral simulations. Simulation of variable-temperature $^{31}\text{P}\{^1\text{H}\}$ NMR spectra was performed using gNMR5.1. Coupling constants and limiting chemical shifts were determined from a low temperature, “static” spectrum. Coupling constants were treated as constant in the simulations, however, pronounced temperature effects on the chemical shift were noted. Chemical shifts were therefore corrected iteratively in the simulations, using as a criterion the assumption that chemical shift varies linearly with temperature. Linewidths used in the simulations were estimated from the linewidths of resonances not involved in a dynamic process over the temperature range studied, and were treated as constant. Association rates were taken to be twice the NMR rate for intramolecular fluxional processes as usual, and as equal to the NMR rate in the intermolecular exchange process in **4(Cl)**.

Acknowledgements

The financial support of EPSRC, grants RG/R37685 and EP/C0005643, is gratefully acknowledged. K. J. S. acknowledges

the award of an EPSRC DTA studentship. F. Al. M. thanks CARA for a Fellowship. The authors are grateful to Prof. Pierre Braunstein, Prof. Bob Tooze of SASOL European Research Laboratory and Dr Graham Eastham of Lucite International for helpful discussions.

References

- 1 A. Bader and E. Lindner, *Coord. Chem. Rev.*, 1991, **108**, 27–110.
- 2 P. Espinet and K. Soulantica, *Coord. Chem. Rev.*, 1999, **193–195**, 499–556.
- 3 G. R. Newkome, *Chem. Rev.*, 1993, **93**, 2067–2089.
- 4 C. S. Slone, D. A. Weinberger and C. A. Mirkin, *Prog. Inorg. Chem.*, 1999, **48**, 233–350.
- 5 Z. Z. Zhang and H. Cheng, *Coord. Chem. Rev.*, 1996, **147**, 1–39.
- 6 A. Scrivanti, M. Bertoldini, V. Beghetto, U. Matteoli and A. Venzo, *J. Organomet. Chem.*, 2009, **694**, 131–136.
- 7 E. Drent, P. Arnoldy and P. H. M. Budzelaar, *J. Organomet. Chem.*, 1994, **475**, 57–63.
- 8 P. Braunstein, *J. Organomet. Chem.*, 2004, **689**, 3953–3967.
- 9 P. Braunstein, F. Naud, A. Dedieu, M. M. Rohmer, A. DeCian and S. J. Rettig, *Organometallics*, 2001, **20**, 2966–2981.
- 10 G. Chelucci, G. Orru and G. A. Pinna, *Tetrahedron*, 2003, **59**, 9471–9515.
- 11 A. Pfaltz and W. J. Drury, *Proc. Natl. Acad. Sci. U. S. A.*, 2004, **101**, 5723–5726.
- 12 G. Helmchen and A. Pfaltz, *Acc. Chem. Res.*, 2000, **33**, 336–345.
- 13 P. J. Guiry and C. P. Saunders, *Adv. Synth. Catal.*, 2004, **346**, 497–537.
- 14 J. Flapper, P. Wormald, M. Lutz, A. L. Spek, P. W. M. N. van Leeuwen, C. J. Elsevier and P. C. J. Kamer, *Eur. J. Inorg. Chem.*, 2008, 4968–4976.
- 15 R. J. Detz, S. A. Heras, R. de Gelder, P. W. M. N. van Leeuwen, H. Hiemstra, J. N. H. Reek and J. H. van Maarseveen, *Org. Lett.*, 2006, **8**, 3227–3230.
- 16 J. Keijsper, P. Arnoldy, M. J. Doyle and E. Drent, *Recl. Trav. Chim. Pays-Bas*, 1996, **115**, 248–255.
- 17 E. Drent, P. Arnoldy and P. H. M. Budzelaar, *J. Organomet. Chem.*, 1993, **455**, 247–253.
- 18 A. Scrivanti, V. Beghetto, M. Zanato and U. Matteoli, *J. Mol. Catal. A: Chem.*, 2000, **160**, 331–336.
- 19 A. Scrivanti, V. Beghetto, E. Campagna and U. Matteoli, *J. Mol. Catal. A: Chem.*, 2001, **168**, 75–80.
- 20 M. T. Reetz, R. Demuth and R. Goddard, *Tetrahedron Lett.*, 1998, **39**, 7089–7092.
- 21 M. L. Clarke, D. J. Cole-Hamilton, D. F. Foster, A. M. Z. Slawin and J. D. Woollins, *J. Chem. Soc., Dalton Trans.*, 2002, 1618–1624.
- 22 J. J. M. de Pater, C. E. P. Maljaars, E. de Wolf, M. Lutz, A. L. Spek, B. J. Deelman, C. J. Elsevier and G. van Koten, *Organometallics*, 2005, **24**, 5299–5310.
- 23 U. Matteoli, A. Scrivanti and V. Beghetto, *J. Mol. Catal. A: Chem.*, 2004, **213**, 183–186.
- 24 A. Dervisi, P. G. Edwards, P. D. Newman and R. P. Tooze, *J. Chem. Soc., Dalton Trans.*, 2000, 523–528.
- 25 A. Dervisi, P. G. Edwards, P. D. Newman, R. P. Tooze, S. J. Coles and M. B. Hursthouse, *J. Chem. Soc., Dalton Trans.*, 1999, 1113–1120.
- 26 A. Dervisi, P. G. Edwards, P. D. Newman, R. P. Tooze, S. J. Coles and M. B. Hursthouse, *J. Chem. Soc., Dalton Trans.*, 1998, 3771–3776.
- 27 A. Scrivanti, V. Beghetto, E. Campagna, M. Zanato and U. Matteoli, *Organometallics*, 1998, **17**, 630–635.
- 28 S. Doherty, J. G. Knight and M. Betham, *Chem. Commun.*, 2006, 88–90.
- 29 V. K. Jain, V. S. Jakkal and R. Bohra, *J. Organomet. Chem.*, 1990, **389**, 417–426.
- 30 T. Suzuki, M. Kita, K. Kashiwabara and J. Fujita, *Bull. Chem. Soc. Jpn.*, 1990, **63**, 3434–3442.
- 31 J. P. Farr, M. M. Olmstead, F. E. Wood and A. L. Balch, *J. Am. Chem. Soc.*, 1983, **105**, 792–798.
- 32 M. M. Olmstead, A. Maisonnat, J. P. Farr and A. L. Balch, *Inorg. Chem.*, 1981, **20**, 4060–4064.
- 33 C. G. Arena, D. Drommi and F. Faraone, *Tetrahedron: Asymmetry*, 2000, **11**, 4753–4759.
- 34 C. G. Arena, E. Rotondo, F. Faraone, M. Lanfranchi and A. Tiripichio, *Organometallics*, 1991, **10**, 3877–3885.
- 35 J. P. Farr, M. M. Olmstead and A. L. Balch, *J. Am. Chem. Soc.*, 1980, **102**, 6654–6656.
- 36 J. P. Farr, M. M. Olmstead and A. L. Balch, *Inorg. Chem.*, 1983, **22**, 1229–1235.
- 37 J. P. Farr, F. E. Wood and A. L. Balch, *Inorg. Chem.*, 1983, **22**, 3387–3393.
- 38 A. Maisonnat, J. P. Farr, M. M. Olmstead, C. T. Hunt and A. L. Balch, *Inorg. Chem.*, 1982, **21**, 3961–3967.
- 39 A. Maisonnat, J. P. Farr and A. L. Balch, *Inorg. Chim. Acta*, 1981, **53**, L217–L218.
- 40 A. L. Balch, *Adv. Chem.*, 1982, **196**, 243–255.
- 41 P. E. Garrou, *Chem. Rev.*, 1981, **81**, 229–266.
- 42 G. R. Newkome, D. W. Evans and F. R. Fronczek, *Inorg. Chem.*, 1987, **26**, 3500–3506.
- 43 Y. Xie, C. L. Lee, Y. P. Yang, S. J. Rettig and B. R. James, *Can. J. Chem.*, 1992, **70**, 751–762.
- 44 The presence of strong pyridyl ligand vibrations in the IR spectrum masks the Pd–Cl vibrations that could otherwise be used to confirm the presence or absence of a mixture of complexes in the solid. see ref. 43.
- 45 M. M. Olmstead, R. R. Guimerans, J. P. Farr and A. L. Balch, *Inorg. Chim. Acta*, 1983, **75**, 199–208.
- 46 J. A. Casares, P. Espinet and G. Salas, *Chem.–Eur. J.*, 2002, **8**, 4843–4853.
- 47 A. Bondi, *J. Phys. Chem.*, 1964, **68**, 441.
- 48 A. Mendia, E. Cerrada, F. J. Arnaiz and M. Laguna, *Dalton Trans.*, 2006, 609–616.
- 49 A. Cingolani, Effendy, D. Martini, C. Pettinari, B. W. Skelton and A. H. White, *Inorg. Chim. Acta*, 2006, **359**, 2183–2193.
- 50 J. K. Liu, B. T. Heaton, J. A. Iggo and R. Whyman, *Angew. Chem., Int. Ed.*, 2004, **43**, 90–94.
- 51 J. Liu, B. T. Heaton, J. A. Iggo and R. Whyman, *Chem. Commun.*, 2004, 1326–1327.
- 52 G. P. C. M. Dekker, C. J. Elsevier, K. Vrieze and P. W. N. M. van Leeuwen, *Organometallics*, 1992, **11**, 1598–1603.
- 53 J. K. Liu, B. T. Heaton, J. A. Iggo, R. Whyman, J. F. Bickley and A. Steiner, *Chem.–Eur. J.*, 2006, **12**, 4417–4430.
- 54 W. Clegg, G. R. Eastham, M. R. J. Elsegood, B. T. Heaton, J. A. Iggo, R. P. Tooze, R. Whyman and S. Zacchini, *J. Chem. Soc., Dalton Trans.*, 2002, 3300–3308.
- 55 A. V. Kulik, L. G. Bruk, O. N. Temkin, V. R. Khabibulin, V. K. Belsky and V. E. Zavodnik, *Mendeleev Commun.*, 2002, **12**, 47–48.
- 56 Z. Y. Lin and M. B. Hall, *Inorg. Chem.*, 1991, **30**, 646–651.
- 57 U. Frey, L. Helm, A. E. Merbach and R. Romeo, *J. Am. Chem. Soc.*, 1989, **111**, 8161–8165.
- 58 R. Romeo, *Comments Inorg. Chem.*, 1990, **11**, 21–57.
- 59 R. Romeo, A. Grassi and L. M. Scolaro, *Inorg. Chem.*, 1992, **31**, 4383–4390.
- 60 J. A. Casares, S. Coco, P. Espinet and Y. S. Lin, *Organometallics*, 1995, **14**, 3058–3067.
- 61 A. L. Casado, A. A. Casares and P. Espinet, *Inorg. Chem.*, 1998, **37**, 4154–4156.
- 62 R. G. Wilkins, in *Kinetics and Mechanism of Reactions of Transition Metal Complexes*, Wiley-VCH Verlag GmbH & Co., Weinheim, 2nd edn, 2003, pp. 199–256.
- 63 S. Q. Niu and M. B. Hall, *Chem. Rev.*, 2000, **100**, 353–405.
- 64 Z. Chval, M. Sip and J. V. Burda, *J. Comput. Chem.*, 2008, **29**, 2370–2381.
- 65 K. Tatsumi, R. Hoffmann, A. Yamamoto and J. K. Stille, *Bull. Chem. Soc. Jpn.*, 1981, **54**, 1857–1867.
- 66 J. P. Stambuli, C. D. Incarvito, M. Buhl and J. F. Hartwig, *J. Am. Chem. Soc.*, 2004, **126**, 1184–1194.
- 67 A. C. Albéniz, A. L. Casado and P. Espinet, *Inorg. Chem.*, 1999, **38**, 2510–2515.
- 68 T. Ukai, H. Kawazura, Y. Ishii, J. J. Bonnet and J. A. Ibers, *J. Organomet. Chem.*, 1974, **65**, 253–266.
- 69 M. S. Kharasch, R. C. Seyler and F. R. Mayo, *J. Am. Chem. Soc.*, 1938, **60**, 882–884.